Thesis Title: Characterizing Senescence Induction and Senolytic Sensitivity in Murine Lung Cancer Cell Lines

By:

Rana Estaleen

Advisor: Dr. David Gewirtz

Advisory Committee: Dr. David Gewirtz, Dr. Imad Damaj, and Dr. Santiago Lima

May 10, 2022

A thesis submitted in partial fulfillment of the requirements for the degree of Master of Science at Virginia Commonwealth University

Table of Contents

Abstract

While cancer patients often experience tumor reduction after receiving chemotherapy, tumors can eventually emerge from a state of dormancy. Cancer cells treated with the topoisomerase II poison, etoposide (ETO), enter senescence, which is a durable and prolonged cell cycle growth arrest. Different murine lung cell lines were screened for their levels of senescence induction by ETO, and those showed promising senescence induction were then treated with the senolytic, ABT263, to promote apoptosis. The hypothesis of this work was that non-small cell lung cancer cell lines will have different degrees of senescence and that the magnitude of the response to senolytics would reflect the extent of senescence induction. An additional goal of this study was to identify an appropriate mouse lung cancer line that could be used to study the interactions with the immune system. X577, E889, X381 and CMT167 cells had different degrees of senescence, and had different degrees of response to the treatment with ABT263. However, there was no clear correlation between the extent of senescence induction and the response to ABT263, and this is assumed to be due to the different genetic makeup of the cells. After analysis of the time to recovery from the treatment with ETO and ABT263, it was determined that X577 cells had the potential be investigated in vivo.

1. Introduction

1.1. Cancer background

Cancer is a disease in which cells undergo mutations that allow them to grow uncontrollably and, in some cases, to metastasize. Cancer is thought to be driven by defects in the host's genes or by defects in gene regulation. Cancer cells differ from normal cells in their ability to sustain proliferative signaling, evade growth suppressors, resist cell death, enable replicative immortality, induce angiogenesis, and activate invasion and metastasis (Hanahan, 2011). According to the NIH, lung cancer is one of the leading causes of new cancer cases in 2021. It was estimated that lung cancer would represent 12.4% of all new cancer cases in the U.S., and, compared to other cancer related deaths, there were going to be 22% lung cancer deaths with the five-year survival rate of 21.7% (NIH, 2021).

1.2. Lung cancer background

There are two main types of lung cancer, non-small cell lung cancer (NSCLC) and small cell lung cancer (SCLC). The main subtypes of NSCLC are adenocarcinoma, squamous cell carcinoma, and large cell carcinoma. About 80-85% of lung cancers are NSCLC.

Adenocarcinomas start in cells that normally secrete mucus and they're usually found in the outer parts of the lung and are more likely to be found before they have spread. This cancer occurs mainly in people that smoke or used to smoke; it is also the most common type of lung cancer seen in people who don't smoke. It is more common in women than in men, and it is more likely to occur in younger people than other types of lung cancer.

Squamous cell carcinomas start in squamous cells, which are flat cells that line the inside of the airways in the lungs and it can be found in the central part of the lungs, near a main airway (bronchus).

Large cell (undifferentiated) carcinomas can appear in any part of the lung, this type of lung cancer tend to grow and spread quickly, which can make it harder to treat.

SCLC tends to grow and spread faster than NSCLC and about 70% of patients with SCLC will have cancer that has already metastasized by the time they are diagnosed. There are two main types of small cell lung cancer, small cell carcinoma and combined small cell carcinoma. Chemotherapy and radiation therapy work best at treating SCLC because of how fast it grows. Unfortunately, for most people, the cancer will return at some point.

There are different treatments for NSCLC, some of which are, but not limited to, surgery, radiation therapy, chemotherapy, targeted therapy, immunotherapy, laser therapy, photodynamic therapy, cryosurgery, and electrocautery. Small cell lung cancer has six types of standard treatments: surgery, chemotherapy, radiation therapy, immunotherapy, laser therapy, and endoscopic stent placement.

1.3. Chemotherapy treatment

Chemotherapy uses drugs to stop the growth of cancer cells, either by killing the cells or by stopping the cells from dividing. Chemotherapy can be used to cure cancer, lessen the chance it will return, or stop or slows its growth. It can be used to shrink tumors in patients that experience pain and other problems from cancer. Systemic chemotherapy is chemotherapy that is taken orally, injected intravenously or intramuscularly. Regional chemotherapy is chemotherapy placed directly into the cerebrospinal fluid, an organ, or a body cavity such as the abdomen. Chemotherapy drugs can be used alone or in combination with other chemotherapy drugs or immunotherapy. Chemotherapy is used with other cancer treatments to decrease the size of tumor before surgery, kill cancer cells that may remain after surgery or radiation therapy, kill

cancer cells that have returned or metastasized to other parts in the body, or help other chemotherapy drugs work better.

According to the American Cancer Society, chemotherapeutic drugs can cause side effects, the magnitude of which depend on the type and dose of drugs given and how long they are taken. Some side effects examples are, but not limited to, hair loss, mouth sores, loss of appetite or weight changes, nausea and vomiting, and diarrhea or constipation. Chemotherapeutic drugs can also affect the bone marrow blood-forming cells and can lead to increased chance of infections, easy bruising or bleeding, and fatigue. These side effects usually subside after treatment is finished. Although patients can be given drugs that can help prevent or reduce nausea and vomiting (American, 2020), there are no available treatment for other serious side effects such as peripheral neuropathy, chemo-brain, renal damage from platinum based drugs, and cardiotoxicity of drugs such as doxorubicin.

A two-step treatment of chemotherapy can slow down the growth of cancer and drive the tumors to cell death giving the patient a longer remission period or suppressing cancer recurrence. The two-step approach we have been studying is the induction of senescence followed by the use of senolytics.

1.4. Senescence

Senescence is a durable and prolonged growth arrest by which cancer cells can escape chemotherapy-induced death (Sharpless et. al., 2015). Senolytics are a drug class that targets and kills senescent cells (Dorr et. al., Xu et. al., Zhu et. al., 2013). Senescence induction by different stimuli share some common characteristics including an essentially stable growth arrest, relative resistance to apoptosis, persistent DNA damage signaling, changes in heterochromatin, decreased lamin B1 levels, and increased expression of the cyclin-dependent kinase inhibitors, p16, p21 and senescence-associated β-galactosidase (SA-β-gal). Senescent cells secrete proinflammatory cytokines, chemokines, matrix metalloproteinases bioactive lipids, noncoding nucleotides, vesicles, and growth factors, collectively termed the senescence-associated secretory phenotype (SASP) (Prasanna et. al., 2021).

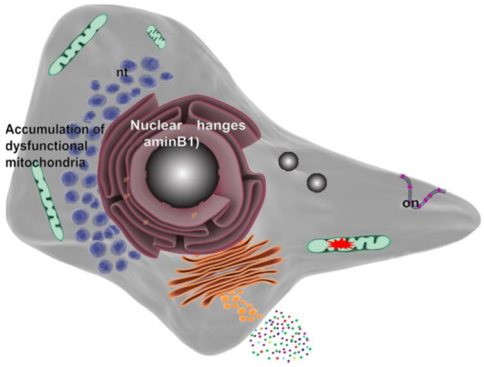

Senescence induction can also occur in tumor cells by targeted chemotherapy. Figure on the right illustrates the phenotype of senescent cells appears as macro-molecular

damage, dysregulated metabolism, apoptosis resistance, and a secretome which has diverse inflammatory mediators, growth factors, and different enzymes called the senescence-associated secretory phenotype (SASP) (Hernandez-Segura et. al., 2018).

There are different types of senescence: DNA damage-induced senescence, oncogene-induced senescence, oxidative stress-induced senescence, chemotherapy-induced senescence, mitochondrial dysfunction-associated senescence, epigenetically induced senescence, paracrine senescence, and replicative senescence (Hernandez-Segura et. al., 2018).

DNA damage-induced senescence occurs when DNA is damaged and this damage can induce either senescence or apoptosis, depending on how damaged the DNA is (Hernandez-Segura et. al., 2018; Munoz-Espin, 2014). Oncogene-induced senescence occurs by the activation of oncogenes, such as Ras, or the inactivation of tumor suppressors, such as PTEN (Hernandez-Segura et. al., 2018; Munoz-Espin, 2014; Sharpless et. al., 2015). Chemotherapy-induced senescence occurs after the use of multiple anticancer drugs, such as the topoisomerase II poison, ETO, which induce DNA damage, and others that can act through different mechanisms, such as the inhibition of pro-survival proteins like the BCL_2 family (Saleh et.al., 2020). Epigenetically induced senescence occurs with the use of DNA methylase inhibitors, such as 5-asa-2'-deoxycytudine, or histone deacetylases inhibitors, such as sodium butyrate (Petrova et. al., 2016). Paracrine senescence is induced by the SASP produced by a primary senescent cell (Acosta et. al., 2013). Replicative senescence occurs when there is a decrease in proliferation potential after multiple cell division that eventually lead to total arrest (Hernandez-Segura et. al., 2018), which is the shorting of telomeres as a consequence of multiple cell divisions in non-transformed cells (Sharpless et. al., 2015).

ETO was the first agent recognized as a topoisomerase II (topo II) inhibiting anticancer drug. In 1983, the FDA approved ETO as a cancer treatment in clinical settings (Hande, 1998). ETO, is converted to O-demethylated metabolites, in a reaction that is mediated by CYP3A4 and CYP3A5; the metabolites have similar potency at inhibiting topoisomerase II as the parent compound. The parent drug, ETO, and its metabolites stabilize the double-stranded DNA cleavage normally catalyzed by topoisomerase II (topo II) and inhibit the religation of DNA breaks. These double-strand DNA breaks subsequently trigger the desired antitumor effects which is cell death, but can also be senescence (Yang, et. al., 2009).

Induction of cellular senescence is a mechanism by which cancer therapies exert antitumor activity and tumor stasis. Conversely, there is an increasing amount of evidence from preclinical studies shows that radiation and chemotherapy cause accumulation of senescent cells both in tumor and normal tissue. This increase of senescent cells in tumors can promote tumor relapse, metastasis, and resistance to therapy; furthermore, senescent cells in normal tissue can contribute to certain radiation- and chemotherapy-induced side effects (Prasanna et. al. 2021).
After senescence induction, cells can recover from senescence, and re-emerge into an actively proliferating state (Chakradeo et. al., 2016; Saleh et. al., 2020). Although, the recovery process is unclear, we believe that it can be from previously senescent cells, cells in growth arrest from quiescent, or cells that are resistant to treatment. The senescent cells are in growth arrest; however, a portion of the cell population may die. When the cells that have entered into senescence are treated with a senolytic, a portion of the senescent cell population are targeted for cellular death; this would leave some cells, those that did not enter senescence and those that could resist the senolytic treatment, alive. The surviving cells will eventually grow and proliferate as previously and even more aggressively than before because those cells are considered to be drug resistant. This recovery phenomenon is seen in patients with cancer; they are treated with chemotherapy and the treatment works for a period of time, which can be months or years, and suddenly the cancer reoccurs more rigorous and aggressive than before. This indicates that the use of senolytics is vital in regards to the clearance of the senescent cells.

1.5. Apoptosis

Apoptosis is a programmed cell death pathway that is associated with a set of biochemical and physical changes involving the nucleus, the cytoplasm, and the plasma membrane. During the early stages of apoptosis, the cells round up and shrink. In the cytoplasm, the endoplasmic reticulum dilates and the cisternae swell to form vesicles and vacuoles. In the nucleus, chromatic condenses and accumulate into dense compact masses and is fragmented internucleosomally by endonucleases. The nucleus becomes convoluted and buds off into several fragments, which are encapsulated within the forming apoptotic bodies. In the plasma membrane, cell junctions are disintegrated and the plasma membrane becomes gets twisted around and eventually starts to make a rounded outgrowth on the surface of the cell. The cell can then break up in an elaborate manner which will lead to the falling away of several membrane spheres containing the packaged cellular contents; this is identified as apoptotic bodies of various sizes (Lawen, 2003).

1.6. Senolytics

Senescent cells express prosurvival proteins that block apoptosis, such as BCL_2 and BCL_{XL} (Chang et. al., 2016; Short et. al., 2019; Wang et. al., 2017). Senotherapeutics are a new drug class that selectively kill senescent cells, which are known as senolytics (Saleh et. al., 2020; Short et. al., 2019). During the last decade, several senolytics have been identified and have been used in clinical trials. Preclinical data implies that senolytics alleviate disease in numerous organs, improve physical function and resilience, and suppress all causes of mortality (Robbins, et. al., 2020). Different senolytics were investigated for this study. ABT263, navitoclax, ABT199, and A1155463 are BH3 mimetics which prevent the BCL2 family proteins from inhibiting the action of pro-apoptotic proteins. Upon activation, the pro-apoptotic proteins permeate the mitochondria, allowing cytochrome C release into the cytoplasm where it binds and activate the apoptotic protease activating factor-1 allowing its binding to ATP and the formation of the apoptosome resulting in the activation of caspase-3 and finally cellular apoptosis (Zhan et. al., 2019). Another senolytic is ARV525, which is a BET family protein degrader, that is thought to produce senolysis by targeting NHEJ and autophagy in senescent cells (Wakita, et. al., 2020).

1.7. Preliminary data and research introduction

The human lung cancer cell line, A549, was shown in our laboratory to undergo senescence upon treatment with ETO, and to die upon exposure to the senolytic agent, ABT263, both in vitro and in vivo (Saleh et. al.). However, these studies were performed in an immune deficient animal that would not reject the human tumor cells. In order to identify a mouse cell line to study the interaction of the immune system when treated with ETO and ABT263, mouse lung cancer cell lines, including CMT167, with different genetic backgrounds (Noland et. al., 2011) were investigated.

Senescence induction was monitored based on the upregulation of the lysosomal content, β-galactosidase expression, as well as the upregulation of Cathepsin D1, p21, p53, and the down regulation of Lamin B1. Cells that responded to ETO by undergoing senescence were then tested with senolytics, including ABT263, and ARV825.

ABT263 is a senolytic which targets the BCL2 family (Zhan et. al., 2019). ABT263 has shown to be toxic when used in large doses (Zhan et. al., 2019); therefore, a less toxic with a more therapeutic index drug, AZD0466, was tested in murine lung cancer lines. AZD0466 is a potent dual BCL_2 /BCL_{XL} inhibitor which can drive cells into apoptosis (Patterson et. al., 2021).

Another drug class is ARV825, which is a BET family protein degrader that provokes senolysis in senescent cells (Wakita et. al., 2020).

2. Methods and Materials

2.1. Cell lines and drug treatments

The six cell lines were provided by researchers at Virginia Commonwealth University: H Li (Y856, X577, X381, E889, X911, and Y143). All cell lines were maintained in DMEM (Thermo Fisher, Waltham, MA, USA) with 10% (v/v) fetal bovine serum (Gemini, West Sacramento, CA, USA), and 100 $U \cdot mL^{-1}$ penicillin G sodium/100 $\mu g \cdot mL^{-1}$ streptomycin sulfate (Thermo Fisher). Etoposide (Sigma-Aldrich, St. Louis, MO, USA), ABT263 (AbbVie) ABT199 (APExBio, Houston TX, USA), A1155463 (APExBio), ARV825 (AbbVie), and AZD0466 (AbbVie) were all dissolved in DMSO and administered in the dark at the desired concentrations.

2.2 SA-β-galactosidase staining and C_{12}FDG quantification

Histochemical staining of SA-β-galactosidase by X-Gal, quantification of SA-β-galactosidase positive cells by C_{12}FDG flow cytometry. For X-Gal staining of cells, cells were fixed and stained. All images taken on an Olympus (Tokyo, Japan) inverted microscope at 20×. For C_{12}FDG, cells were treated with 100 nM bafilomycin for 60 minutes at 37ºC, then 10 μM C_{12}FDG for 2 hours at 37ºC, subsequently, the cells were collected and centrifuged, washed with PBS and re-centrifuged, finally, the pallet was re-suspended in PBS and immediately analyzed with flow cytometry (excitation/emission = 490/514).

2.3 Cell viability

Number of viable cells were obtained by hemocytometer at various time points during and/or after treatment. Media was replenished every 48 hours. Non-viable cells were aspirated and only viable cells were counted.

2.4. Antibodies

The following primary antibodies were used: cleaved caspase 3 (Cell Signaling, Danvers, MA, USA. Cat. Num.: 9664S), BCL_{XL} (Cell Signaling. Cat. Num.: 2764S), BCL_2 (Abcam, Cambridge, UK. Cat. Num.: GR249198-74), BCL_W (Cell Signaling. Cat. Num.: 2724S) Bax (Cell Signaling. Cat. Num.: 2772S), Bak (Cell Signaling. Cat. Num.: 12105S), Lamin B1 (Cell Signaling. Cat. Num.: 12586S), β-actin (Cell Signaling. Cat. Num.: 4976S), Bim (Cell Signaling. Cat. Num.: 2933S), Cathepsin D (Cell Signaling. Cat. Num.: 2248S), Noxa (Cell Signaling. Cat. Num.:14766S), P21(Santa Cruz Biotechnology, Santa Cruz, CA, USA. Cat. Num.: SC-397), P53

(Cell Signaling. Cat. Num.: 9282S). The secondary antibody used was anti-rabbit IgG (Cell Signaling. Cat. Num.: 7074S).

2.5. Annexin-V/PI and APC Annexin-V/7-AAD apoptosis staining

Apoptosis quantification, based on Annexin-V/PI (BD Biosciences, San Diego, CA, USA) or APC Annexin-V/7-AAD (BioLegend, San Diego, CA, USA) by flow cytometry were conducted by collecting supernatant and cells then centrifuge. Wash pallet with PBS and re-centrifuge. Suspend pellet in 106 µL of staining buffer (per sample: 100 µL 1X Annexin-V Binding Buffer, 3 µL propidium iodide, and 3 µL FITC Annexin-V). Cells expressing GFP were stained with APC Annexin V (per sample: 100 µL 1X Annexin-V Binding Buffer, 3 µL APC Annexin-V, and 3 µL 7-AAD). Cell were stained for 15 minutes at room temperature and analyzed by flow cytometry immediately.

2.6. Western blotting

After the indicated treatments, cells were lifted from the culture plates, collected, and lysed using M-PER mammalian protein extraction reagent (Thermo Scientific, McAllen, TX, USA) containing protease and phosphatase inhibitors (Sigma Aldrich). Protein concentrations were determined by the Bradford assay (Bio-Rad Laboratories). Total protein was then diluted in SDS sample buffer and dry boiled for 5-10 minutes. Protein samples were subjected to SDS-polyacrylamide gel electrophoresis, transferred to polyvinylidene difluoride membrane, and blocked in 5% FBS, 1x PBS, 0.1% Tween 20 (Fisher) for 2 hours. Primary antibodies used at a 1:1000 dilution except for BCL_2 1:2000 dilution and β-actin 1:4000 dilution with overnight incubation in 4^{o}C, followed by extensive washing with Tween-PBS (PBS with 0.1% Tween 20). The membrane was then incubated with secondary antibody of horseradish peroxidase-conjugated goat anti-rabbit IgG antibody (1:2000) for 2 hours at room temperature or overnight in 4^{o}C, followed by extensive washing with Tween-PBS (PBS with 0.1% Tween 20). Blots were developed using Pierce enhanced chemiluminescence reagents (Thermo Fisher Scientific).

2.7. Statistical analysis

Quantitative data are shown as mean ± SEM from at least three independent experiments, which were performed in triplicates. For statistical analysis, GraphPad Prism 8 software (San Diego, CA, USA) was used. Statistical data were analyzed using one- or two-way ANOVA unless otherwise indicated.

3. Results

To disclose past research on lung cancer, figures 1, 2, 3 were adapted from studies by Valerie Carpenter with her permission.

3.1 Senescence induction in A549, a non-small human lung cancer cell line, *in vitro*.

Cellular senescence is "a well-established, highly-programmed response to various DNA damaging antitumor modalities wherein a cancer cell enters into a durable and prolonged growth arrest" (Saleh et al., 2019). ETO, which inhibits topoisomerase II, is used in the treatment of non-small cell lung cancer. Human non-small-cell lung carcinoma (NSCLC) cells (A549) were treated with ETO at a concentration of 8.7 μM for 72 hours, based on pharmacokinetic data (Smyth et. al.). Figure 1A illustrates the promotion of senescence by ETO based on the increased SA-β-gal activity by X-gal and C_{12}FDG. Another marker of senescence is the degradation of Lamin B1, which is shown in figure 1B.

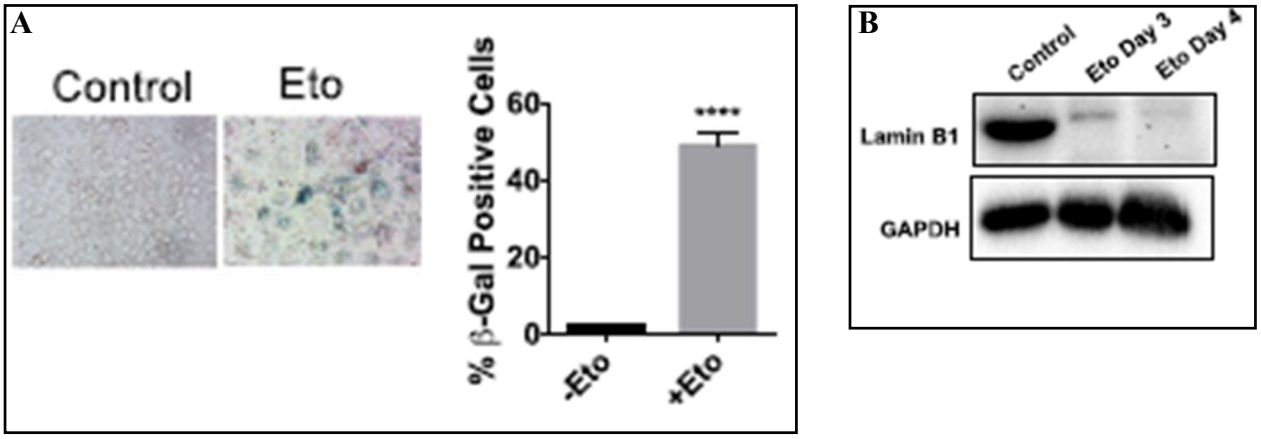

Fig. 1. Etoposide induced senescence in human lung cancer cells, A549. Etoposide A549 cells were exposed to etoposide at a concentration of 8.7 μM for 72 hours. (A) A549 cells were assessed for increased expression of SA-β-gal using X-gal (bright-field images, objective 20x) or C_{12}FDG (bar graph). ****P < 0.0001 indicates statistical significance of treated condition compared to controls as determined using unpaired, Student's *t*-test. (B) Western blotting for Lamin B1 following treatment with etoposide. All images are representative fields or blots from three independent experiments (n = 3), and quantitative graphs are mean ± SEM from three independent experiments (n = 3).

3.2 A549 Sensitivity to the senolytic, ABT263, *in vitro*

Cells induced into senescence by ETO were treated with ABT263 and after the treatment of ABT263, the surviving cells were stained with crystal violet. Figure 2A, shows that treatment with ABT263 resulted in a significant elimination of senescent cells, but not control cells. Figure

2B confirms this finding in a time course study where a single 48-hour treatment with 2 µM ABT263 notably reduced the number of viable cells, but did not affect the non-senescent cells. This indicates that ABT263 only targets senescent cells, and has no effect on the non-senescent cells. It was observed that as ABT263 drives cells toward cell death, its ability to do so, diminishes over time as the cells recover from senescence, which is observed on days 8 to 14 on the cell viability time course in the lower portion of figure 2B.

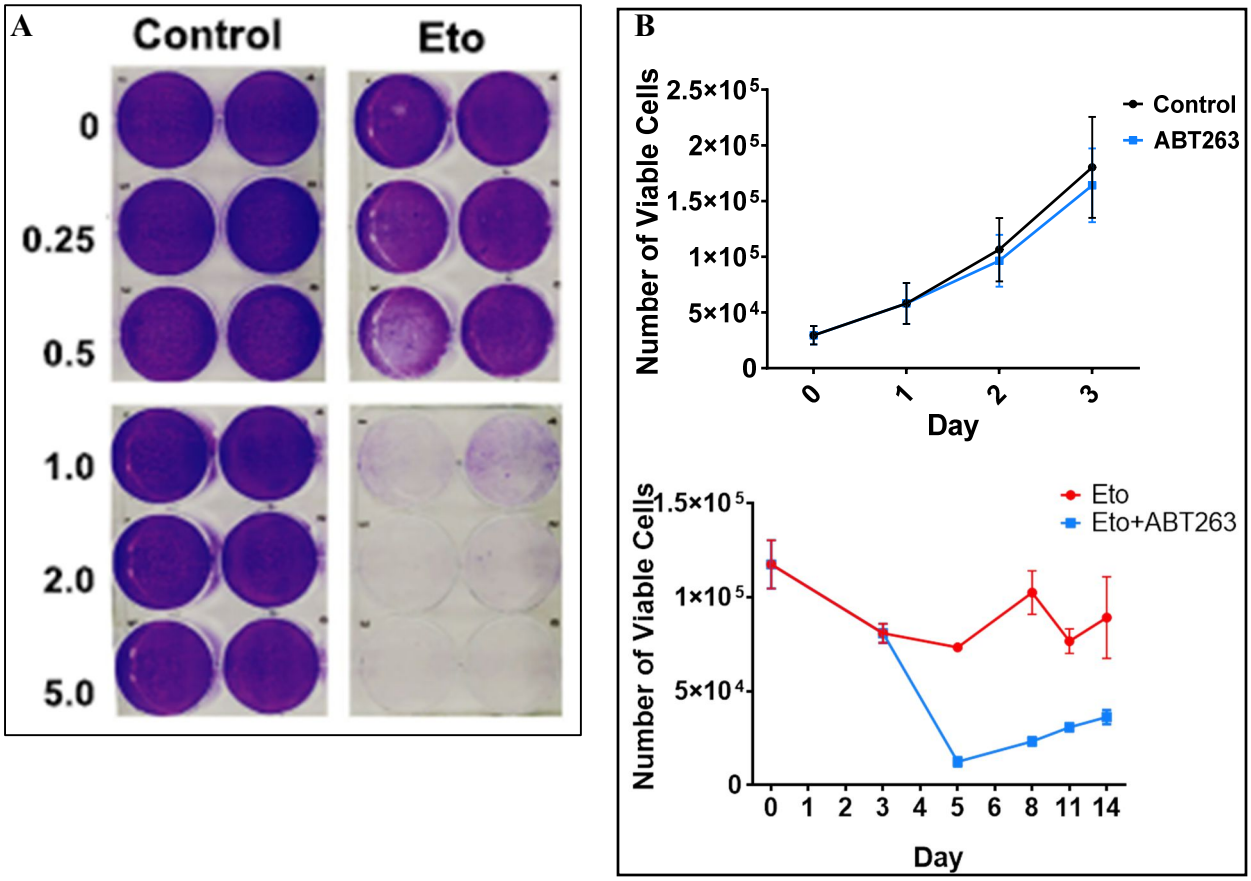

Fig. 2. A549 sensitivity to senolytic ABT263. (A) Crystal violet assay showing a dose response for ABT263. A549 cells were treated with vehicle or 8.7 µM ETO for 72 hrs and then exposed to the indicated concentration of ABT263 for 48 hrs. (B) Cell viability time-courses after treatment of ETO and/or ETO + ABT263. All images are representative images and line graphs are mean ± SEM from at three independent experiments (*n = 3*).

3.3 Senescence induction in the murine lung carcinoma cell line, CMT167

After demonstrating that the A549 human lung cancer cell line, which enters senescence and responds to the senolytic ABT263, a mouse cell line was essential to study the role of the immune system in lung cancer with a two-step treatment, senescence induction and the use of senolytic(s). Seven mouse NSCLC cell lines (CMT167, Y856, X577, X381, E889, Y143, and

X911) were screened for their β-galactosidase (β-gal) levels by X-gal and C12FDG by flow cytometry for quantification of senescence. Figure 3 illustrates the experimental timeline for ETO and ABT263 treatments. To induce senescence, cells were treated on day 0 with 2 μM ETO for 48 hours and were stained with X-gal or C12FDG for β-gal quantification on day 3.

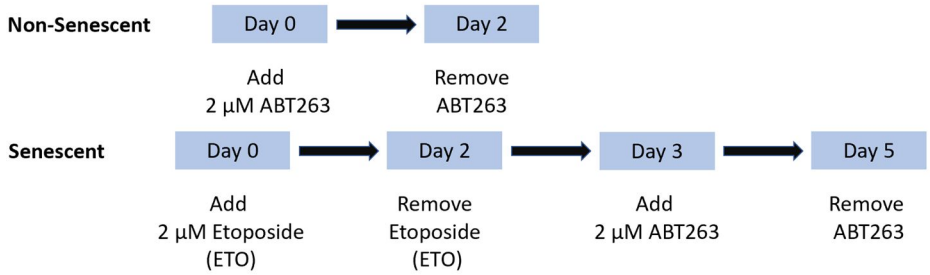

Fig. 3. Experimental timeline for etoposide and ABT263 treatments. Cells were exposed to ETO for 48 hours, for senescence induction, and were placed in DMEM for 24 hours. Cells were then treated with ABT263 for 48 hours. All experimental data collected were collected before, during, and after treatment of ETO and/or ABT263.

Figure 4A presents a dose response for ETO to evaluate the expression of SA-β-gal using X-gal staining. Senescent cells are enlarged, show an altered morphology and green staining due to the upregulation of β-galactosidase. An ABT263 concentration of 2 μM was chosen for further experiments because of the significant increase in staining compared to 0.5 and 1.0 μM, but less cell death than with 5 μM . Figure 4B presents a time course to evaluate senescence induction by 2 μM of ETO, which peaked at 80% on days 3 and 5. To evaluate the senescent cells response to the senolytic, ABT263, day 3 was chosen to treat the cells.

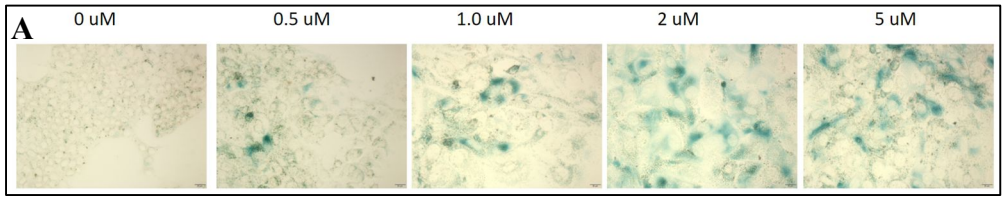

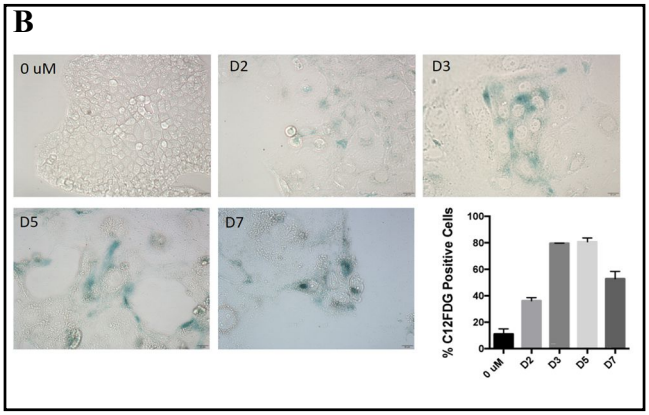

Fig. 4. Etoposide induced senescence in mouse lung cancer cells, CMT167. (A) Cells were exposed to ETO, indicated concentrations, for 48 hrs and evaluated on day 3 for their increased expression of SA-β-gal using X-gal (bright-field images, objective 20X). (B) SA-β-gal time course using 2 μM as the choice of concentration to evaluate the increased expression of SA-β-gal using X-gal (bright-field images, objective 20X) or C_{12}FDG for quantification.

3.4 CMT167 sensitivity to senolytic, ABT263

In order to eliminate cells induced into senescence, a senolytic was screened to target and drive them to apoptosis. The cells induced into senescence by ETO were exposed to ABT263 using the concentrations of 10, 5, 2.5, 1.25, 0.625, 0.3125, and 0 μM (figure 5A) for 48 hours and the surviving CMT167 cells were stained with crystal violet. ABT263 sensitivity was confirmed by performing a cell viability time course using 2 μM of ABT 263. Figures 5B illustrates that ABT263 has no effect on the control cells. As illustrated from the viability time courses (figure 5C) senescent CMT167 cells have a pronounced response to ABT263; however, the effects are transient and after day 7 of ETO treatment, CMT167 cells recovered from senescence; that is, the cells continued to grow. Furthermore, the response to the treatment with ABT263 diminished after day 7 as well. Figure 5C, right panel, when senescent cells escape from senescence, the treatment of ABT263 will no longer be effective. Fig. 5D illustrates a comparison between ETO and ETO + ABT. The treatment with ABT263 reduces cell number on day 5 and on day 14. On day 5, there is a 77.5% reduction in cell viability and on day 14, there is a 23.7% reduction in cell viability.

To determine whether the ABT263 was promoting apoptosis, cell death was assessed by Annexin-V/PI staining and FACS analysis; it was observed that ABT263 drives cells toward apoptosis and there is approximately 50% apoptotic cell death with treatments of ETO followed by ABT263, figure 5E. Annexin V staining specifies how early and late apoptosis is induced in every treatment. In all treatments groups, early apoptosis occurs in more cells than late apoptosis, meaning that the cells were starting the apoptosis process.

3.5. Senescence induction in the syngeneic murine lung cancer cell line, X577

The screening for senescence in the six NSCLC cell lines was chosen on day three because in previous work with the mouse lung cancer line, CMT167, high levels of senescent positive cells were detected after day 3 (Fig. 4B). Figure 6A shows that X577 cells undergo senescence in response to ETO based on the increase of green β-gal staining, cell enlargement and the granulation of cytoplasmic chromatin fragments (CCFs). Figure 6B, β-gal positive cell quantification by flow cytometry, indicates that approximately 37% of the cells have entered into senescence. Figure 6C confirms senescence based on the degradation of Lamin B1. A slight up regulation of Cathepsin D is another marker of senescence, which is also observed. Also, an upregulation of p53 and p21 are an indication of senescence because the cells are in a stressful

environment due to the treatment of ETO. Since the X577 cells demonstrated senescence induction, although less than 40%, sensitivity to ABT263 was assessed.

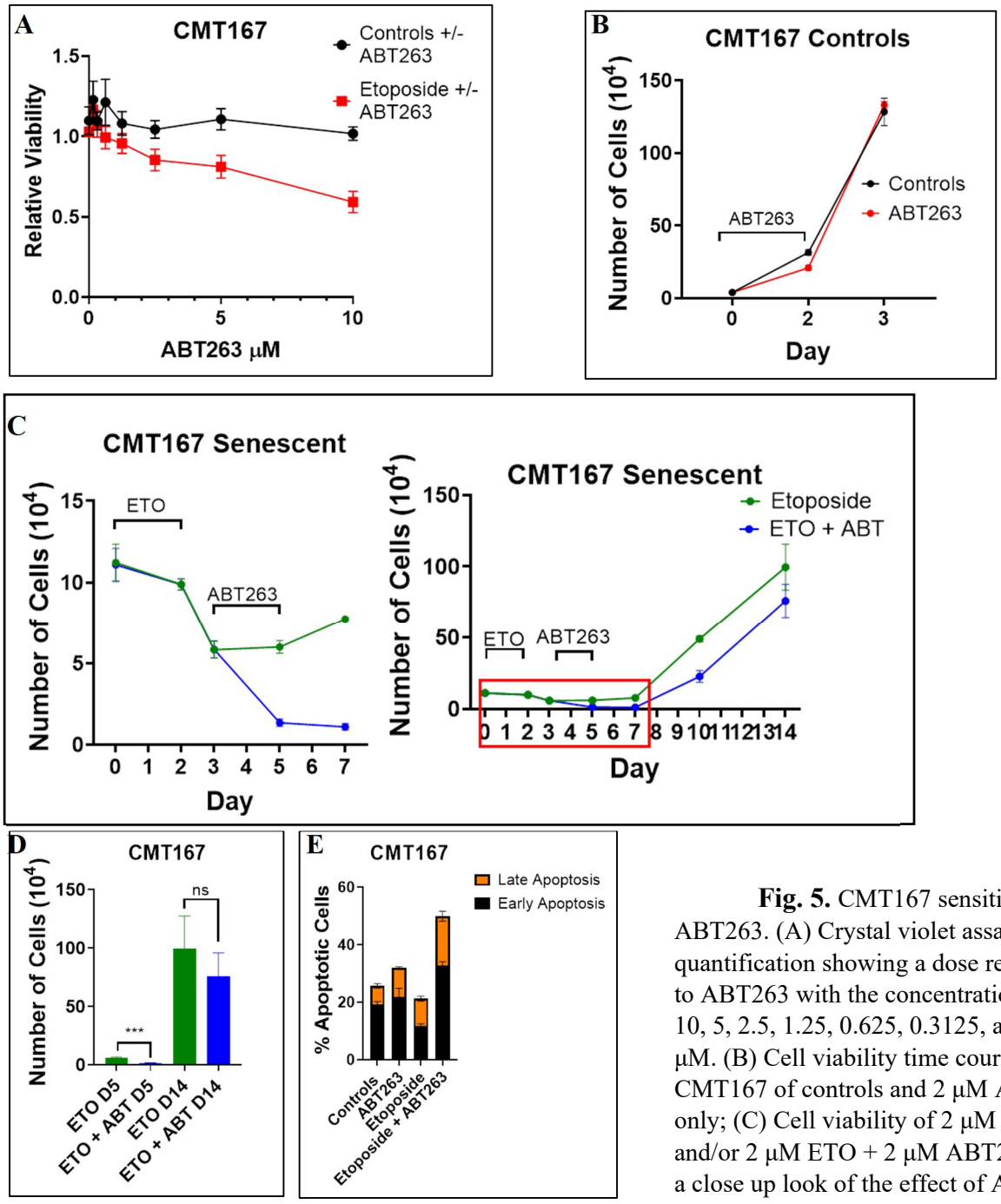

Fig. 5. CMT167 sensitivity to ABT263. (A) Crystal violet assay quantification showing a dose response to ABT263 with the concentrations of 10, 5, 2.5, 1.25, 0.625, 0.3125, and 0 μM. (B) Cell viability time course for CMT167 of controls and 2 μM ABT263 only; (C) Cell viability of 2 μM ETO and/or 2 μM ETO + 2 μM ABT263 and a close up look of the effect of ABT263 to clarify the response of ABT263. (D) A bar graph to compare ETO to ETO + ABT treatments on days 5 and 14. ***$P \leq 0.0005$ indicates statistical significance of treated condition compared to their counterpart as determined using unpaired, Student's *t*-test. (E) Annexin-V/PI quantification of apoptosis induced by 2 μM ABT263 with overnight exposure. Images and line graphs are representative images or graphs from three independent experiments ($n = 3$). Bar graph is mean ± SEM.

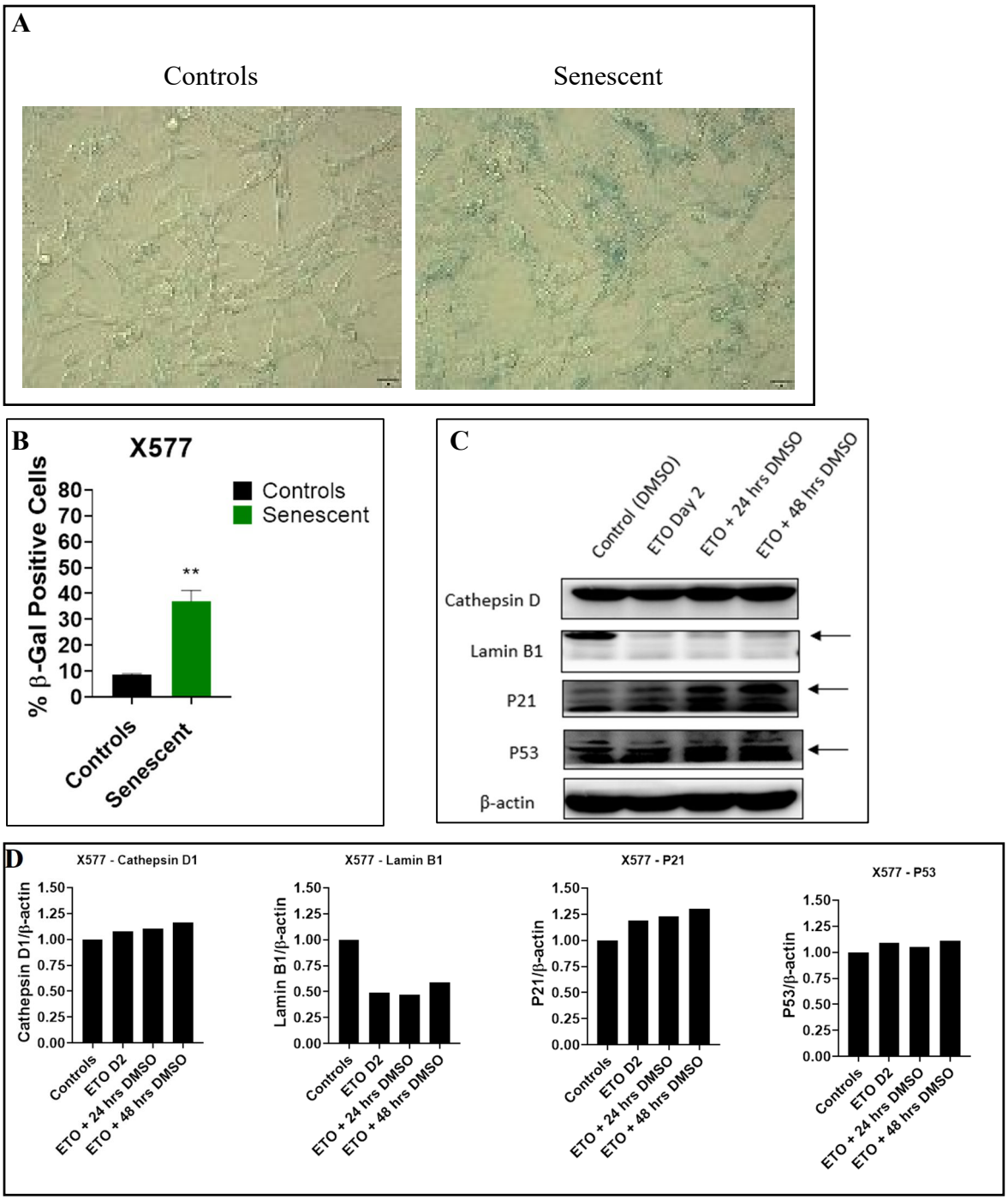

Fig. 6. Etoposide induced senescence in mouse lung cancer X577 cells. Cells were exposed to ETO (2 μM for 48 hrs) and were evaluated for their increased expression of SA-β-gal using (A) X-gal (bright-field images, objective 20X) or (B) C_{12}FDG, the next day. ** $P \leq 0.0026$ indicates statistical significance of treated condition compared to controls as determined using unpaired, Student's *t*-test. (C) Western blotting of Cathepsin D, Lamin B1, P21, and P53 (D) is a quantification of western blots. All images are representative images from three independent experiments ($n = 3$), and quantitative graphs are mean ± SEM from three independent experiments ($n = 3$). Western blots and quantifications are one repeat ($n = 1$).

3.6. X577 sensitivity to ABT263

Figures 7A and 7B and 7D show that X577 cells induced into senescence by ETO responded to ABT263 largely in the same manner as the CMT167 cells. Figure 7A and 7B show a dose response with ABT263 using 5, 2.5, 1.25, 0.625, 0.3125, and 0 μM concentrations. ABT263 has only a modest effect on the control group; however, when cells are induced into senescence with the treatment of ETO followed by ABT-263, there is a significant reduction in cell viability. Figure 7C indicates that control cells treated with ABT263 only show a negligible effect, indicating that ABT263 doesn't affect non-senescent cells. In the senescent viability graph (figure 7D, right panel), it was observed that the treatment with ETO alone induced the cells into senescence until day 7 and that the cells have recovered by day 10. This recovery indicates that after the cells have escaped from senescence, ABT263 effects have diminished. Figure 7E is a comparison of the effects of ETO alone and ETO + ABT263 on days 5 and 10. From cell viability time courses, ABT263 has more efficacious = on X577 cells than on CMT167.
Again, Annexin-V/PI staining as well as western blotting for caspase 3 cleavage were performed to investigate the extent of apoptosis shown in figure 8. As expected, senolytic ABT263 exerts its effects against senescent cells by inducing apoptotic cell death. This is shown by the increase of Annexin-V/PI staining. With controls, there are about 5% apoptotic cells that appear to be in late apoptosis. In cells treated with ABT263 only, there appears to be equal levels of early and late apoptosis that sum up to 7% apoptosis. Cells treated with ETO only, and that have been left in media for 2 days after treatment, have mostly early apoptosis and when including the late apoptotic cells, there is a 20% apoptosis. Furthermore, when cells are treated with ETO for 48 hours and were given 24 hours in media and 24 hours with ABT263, there is an increase in cellular apoptosis and an increase in both late and early apoptosis, indicating that ABT263 drives the cells to cell death through the apoptotic pathway.

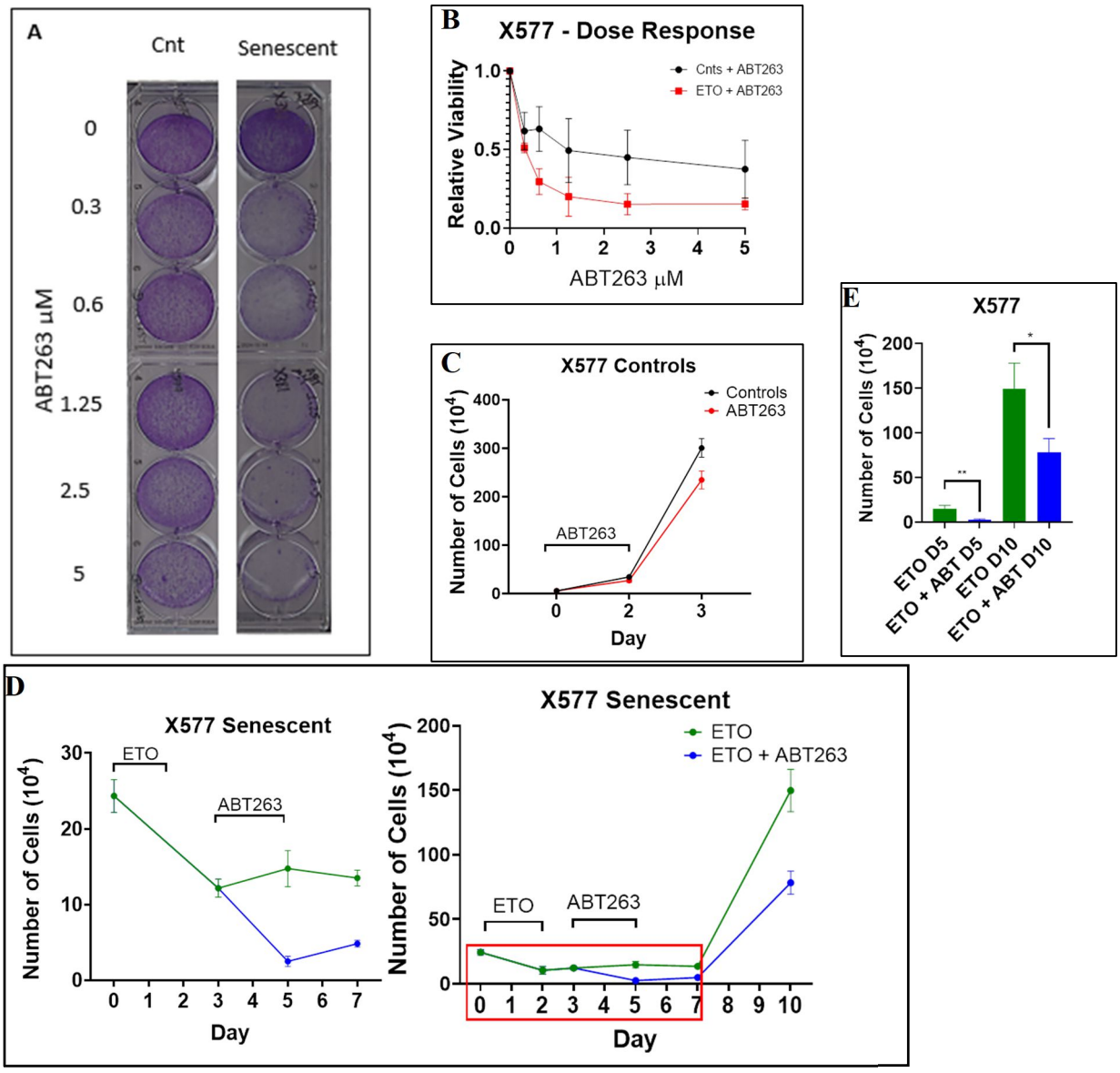

Fig. 7. X577 sensitivity to senolytic ABT263. (A) Crystal violet assay showing a dose response for ABT263. (B) Quantification of the crystal violet using ImageJ. (C) Cell viability time courses for X577 of controls and ABT263 only; (D) Cell viability after treatment of ETO and/or ETO + ABT263 and a close up look of the effect of ABT263 to clarify the response of ABT263. (E) A bar graph to compare ETO to ETO + ABT treatments on days 5 and 10. $^{**}P \leq 0.0078$ and $^{*}P \leq 0.0186$ indicate statistical significance of treated condition compared to their counterpart as determined using unpaired, Student's *t*-test. All images and line graphs are representative images or graphs from three independent experiments ($n = 3$). Bar graph is mean ± SEM from three independent experiments ($n = 3$).

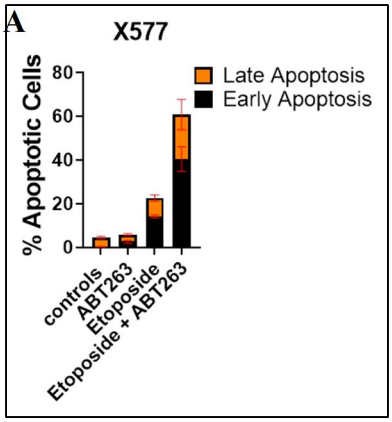

Fig. 8. ABT263 induces apoptotic cell death in senescent cells X577. (A) X577 is Annexin-V/PI quantification of apoptosis induced by 2 μM ABT263 with overnight exposure. Quantification graph is mean ± SEM from three independent experiments (*n = 3*).

3.7. Senescence induction in the syngeneic murine lung cancer cell line, E889

The E889 cell line also shows significance senescent induction with exposure to ETO (figure 9A) with the senescent cells being more granulated and staining for β-gal; β-gal positivity was approximately 44%. To confirm senescence induction after ETO exposure, Cathepsin D1, p21 and p53 levels were investigated using western blotting (figures 9C and D). Figure 9C illustrates the accumulation of Cathepsin D. The upregulation of p21 on day 2 was also observed, however, the protein levels down-regulate on day 3 and 4;, this may indicate that senescence is highest on day 2. There is also, the accumulation of p53 throughout the treatment with ETO.

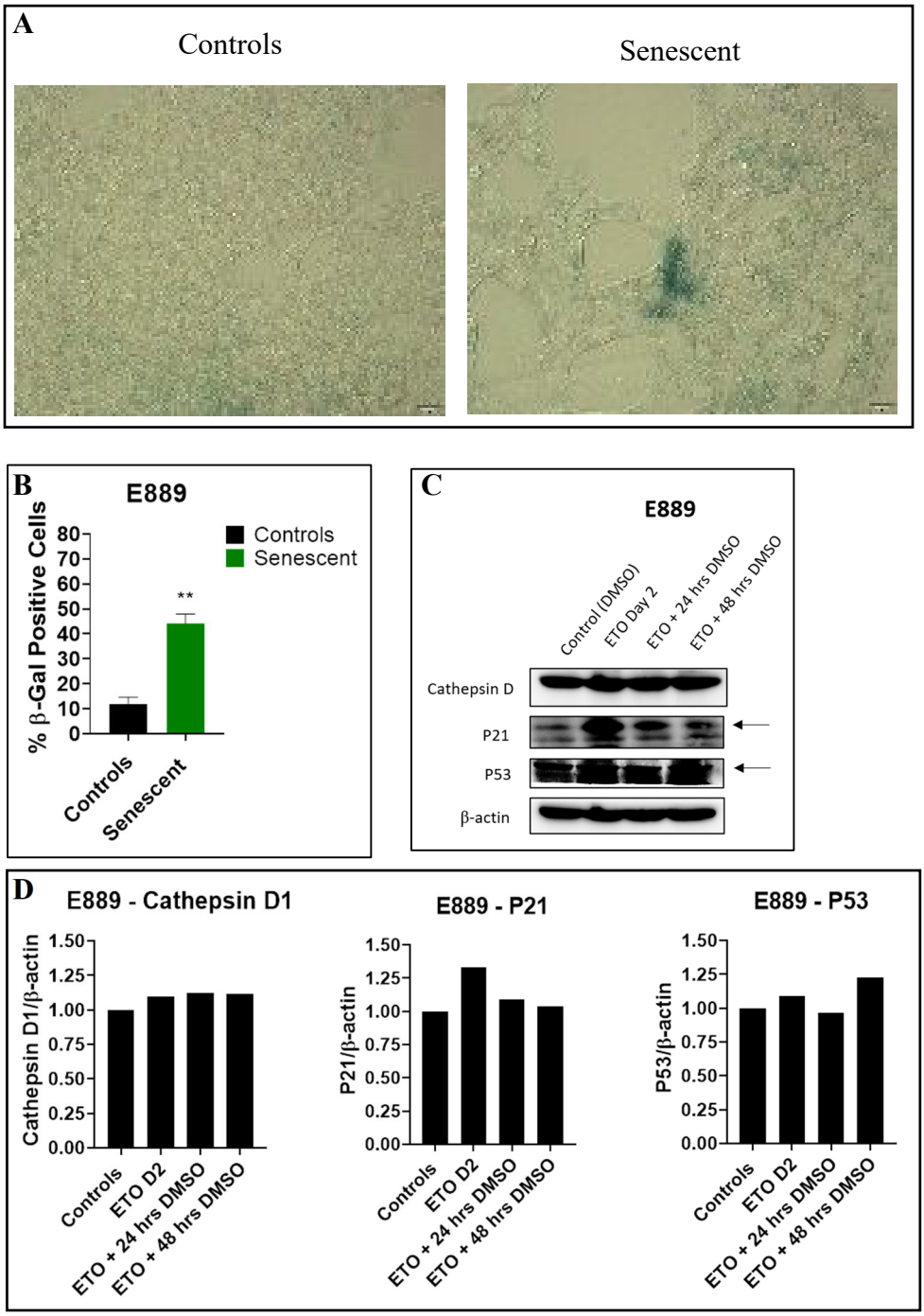

Fig. 9. Etoposide induced senescence in mouse lung cancer E889 cells. Cells were exposed to ETO (2 μM for 48 hrs) and were evaluated for their increased expression of SA-β-gal using (A) X-gal (bright-field images, objective 20X) or (B) C_{12}FDG, the next day. ** $P \leq 0.0023$ indicates statistical significance of treated condition compared to controls as determined using unpaired, Student's *t*-test. (C) Western blotting of Cathepsin D, Lamin B1, P21, and P53 and (D) is western blot quantification. All images are representative images from three independent experiments ($n = 3$), and quantitative graphs are mean ± SEM from three independent experiments ($n = 3$). Western blots and quantifications are one repeat ($n = 1$).

3.8. E889 sensitivity to ABT263

ABT263 reduced the number of E889 senescent cells (Figure 10). Figures 10A and B illustrate that with the treatment of ABT263 only, the cell viability have to some extent was reduced. After the induction of senescence by the exposure to ETO, there was a significant reduction in cell viability after the treatment with ABT263 with 5, 2.5, 1.25, 0.625, 0.3125, and 0 μM doses. Figures 10C illustrates that E889 cells treated with ABT263 alone showed negligible effects.. Figure 10D shows senescence induction after the treatment with ETO. Cells remain arrested between days 0 and 5 and by day 7 the cells start to recover. When the cells are treated with ETO only, there is a reduction in cell viability; this is due to the stress ETO is inducing on the cells. When senescent cells are treated with ABT263, there is a substantial reduction in the cell viability; however, the cells escape from senescence, as the effects of ABT263 is diminished. Figure 10D, right panel, illustrates the recovery of both ETO only and ETO+ABT263 treated cells. Figure 7E is a comparison of the effects of ETO alone and ETO + ABT263 on days 5 and 12. Numbers were acquired from the same time-course for accuracy. The number of cells are reduced on day 5 after treatment of ETO+ABT compared to ETO alone. On day 12, cells treated with ETO+ABT have recovered and have reached the same number of cells as the treatment of ETO. This indicates that after the recovery of senescence the cells will continue to grow.

In E889 cells, ETO treatment reduces the number of viable cells (fig. 10D). Therefore, it was tested with lower doses of ETO (0.5 μM and 1 μM) to observe senescence on days 2, 3, and 5. It was concluded, from X-gal and C12FDG flow cytometry (supp. figs. 1A, B), the lower doses of ETO don't induce senescence as much as 2 μM ETO. And it was decided that the best concentration of ETO is 2 μM.

To further investigate the effects of ABT263, Annexin-APC/7-AAD staining was performed as well as western blotting to monitor the levels of cleaved caspase-3 (figure 11). Senolytic ABT263 exerts its effects against senescent cells by inducing apoptotic cell death. This is shown by the increase of Annexin-V/PI staining. In figures 11B and C, E889 cells undergo apoptosis after the ETO treatment (ETO day 2, 3, and 4), and it shows a significant increase in cleaved caspase 3 after the treatment of both ETO and ABT263. This indicated the increase of apoptosis with the treatment of ETO+ABT263.

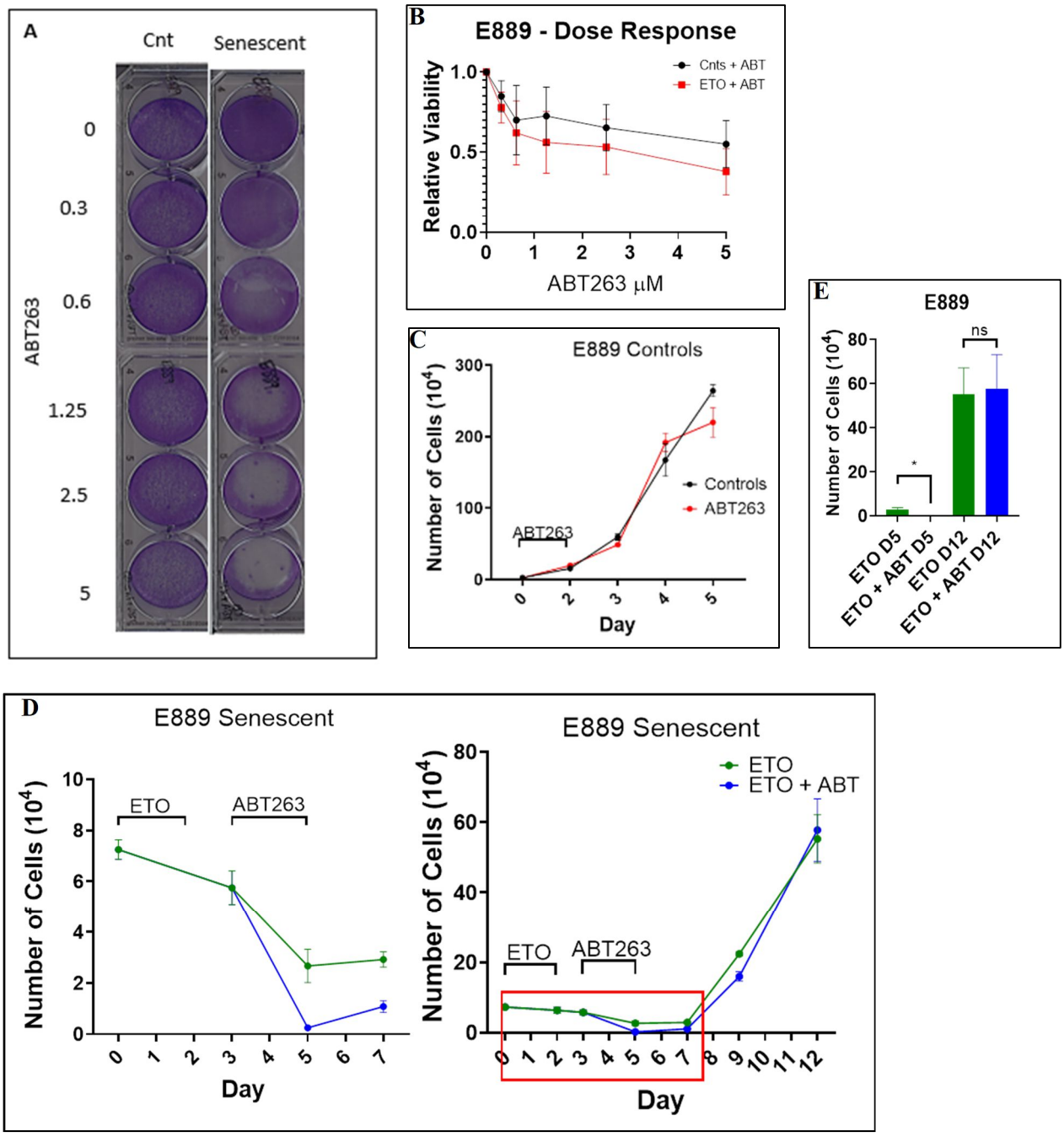

Fig. 10. E889 sensitivity to senolytic ABT263. (A) Crystal violet assay showing a dose response for ABT263. (B) Quantification of the crystal violet using ImageJ. (C) Cell viability time courses for Y856 of controls and ABT263 only; (D) Cell viability after treatment of ETO and/or ETO + ABT263 and a close up look of the effect of ABT263 to clarify the response of ABT263. (E) A bar graph to compare ETO to ETO + ABT treatments on days 5 and 12. * $P \leq 0.0206$ indicates statistical significance of treated condition compared to their counterpart as determined using unpaired, Student's *t*-test. All images and line graphs are representative images or graphs from three independent experiments ($n = 3$). Bar graph is mean ± SEM from three independent experiments ($n = 3$).

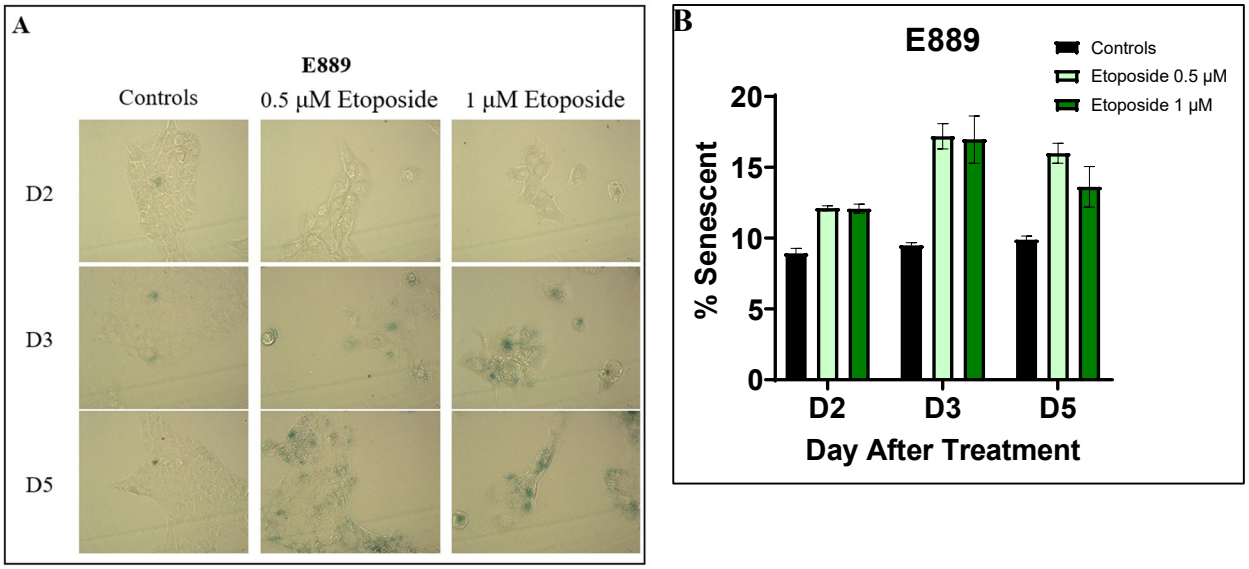

Sup. Fig. 1. Lower doses etoposide induced senescence in E889 cells. Cells were exposed to ETO (0.5 or 1 µM for 48 hrs) and were evaluated for their increased expression of SA-β-gal using X-gal (bright-field images, objective 20X) or C_{12}FDG on days 2, 3, and 5. All images are representative images from three independent experiments (*n = 3*), and quantitative graph is mean ± SEM from two independent experiments (*n = 2*).

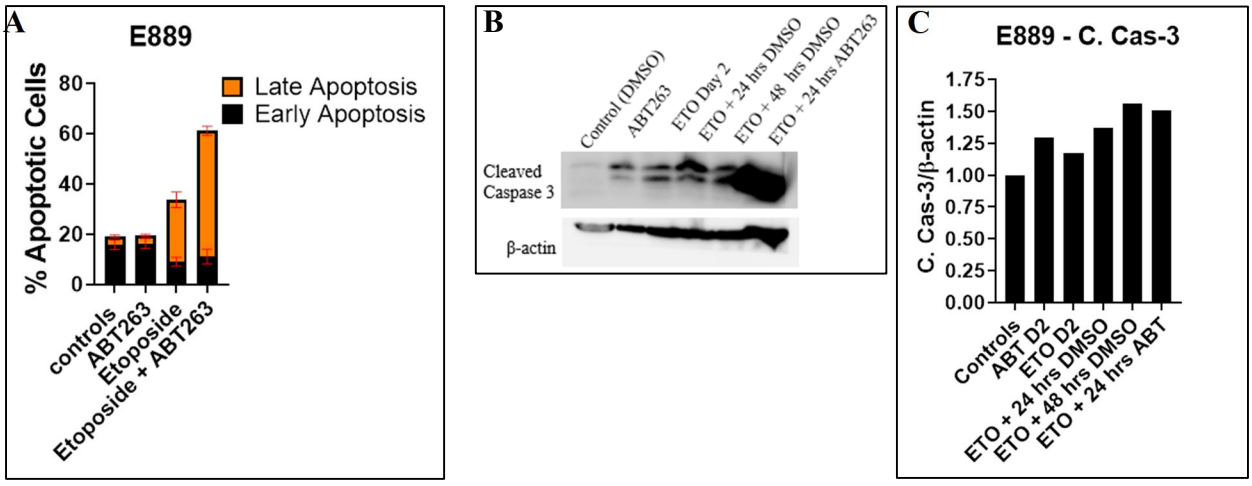

Fig. 11. ABT263 induces apoptotic cell death in senescent cells E889. (A) E889 is Annexin-V/PI quantification of apoptosis induced by 2 µM ABT263 with overnight exposure. (B) Western blotting for cleaved caspase 3 for E889. (C) A bar graph quantification of western blot. Quantification graphs are mean ± SEM from three independent experiments (*n = 3*) and western blots and quantification is one repeat (*n = 1*).

3.9. Senescence induction in the syngeneic murine lung cancer cell line, X381

The X381 cell line also shows significance senescent induction with exposure to ETO (figure 12A) with the senescent cells being more granulated and staining for β-gal; β-gal positivity was approximately 55%. Due to its significant level of β-gal staining and the quantification of β-gal, the effects of ABT263 were investigated with X381 cells.

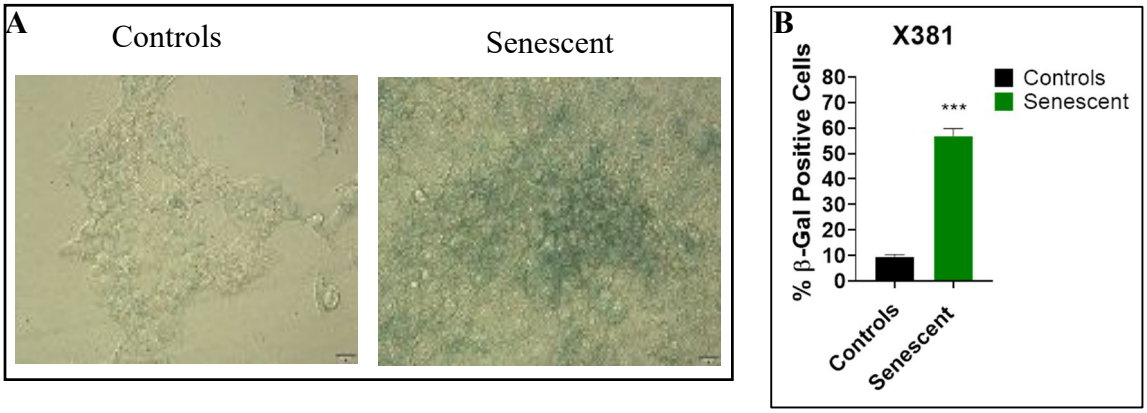

Fig. 12. Etoposide induced senescence in mouse lung cancer X381 cells. Cells were exposed to ETO (2 μM for 48 hrs) and were evaluated for their increased expression of SA-β-gal using (A) X-gal (bright-field images, objective 20X) or (B) C_{12}FDG, the next day. *** $P \leq 0.0001$ indicates statistical significance of treated condition compared to controls as determined using unpaired, Student's *t*-test. All images are representative images from three independent experiments ($n = 3$), and quantitative graphs are mean ± SEM from three independent experiments ($n = 3$).

3.10. X381 sensitivity to ABT263

ABT263 reduced the number of X381 senescent cells (Figure 13). Figures 13A and 13B illustrate that with the treatment of ABT263 alone, the cell viability have to some extent was reduced. After the induction of senescence by the exposure to ETO, there was a significant reduction in cell viability after the treatment with ABT263 with 5, 2.5, 1.25, 0.625, and 0.3125 concentrations .

In the control cells, ABT263 slightly slows down the growth, however, the effect is negligible (figure 13C); in figure 13D, ETO only treated cells were reduced and with the addition of ABT263 the cell viability number continues to decrease. Figure 13C, right panel, indicates that the cells recover from senescence between days 7 and 10. ABT263 killed the senescent cells, and the cells that are left are those that are either resistant to ETO, resistant to ABT263, or both, this may be the reason why the cells treated with ETO+ABT263 have recovered and have surpassed the ETO only treated cells. Figure 13E is a comparison of the effects of ETO alone and ETO + ABT263 on days 5 and 12. Numbers were acquired from the same time-course for accuracy. The

number of cells are reduced on day 5 after treatment of ETO+ABT compared to ETO alone. On day 12, cells treated with ETO+ABT have recovered and have surpassed the number of cells treated with ETO.

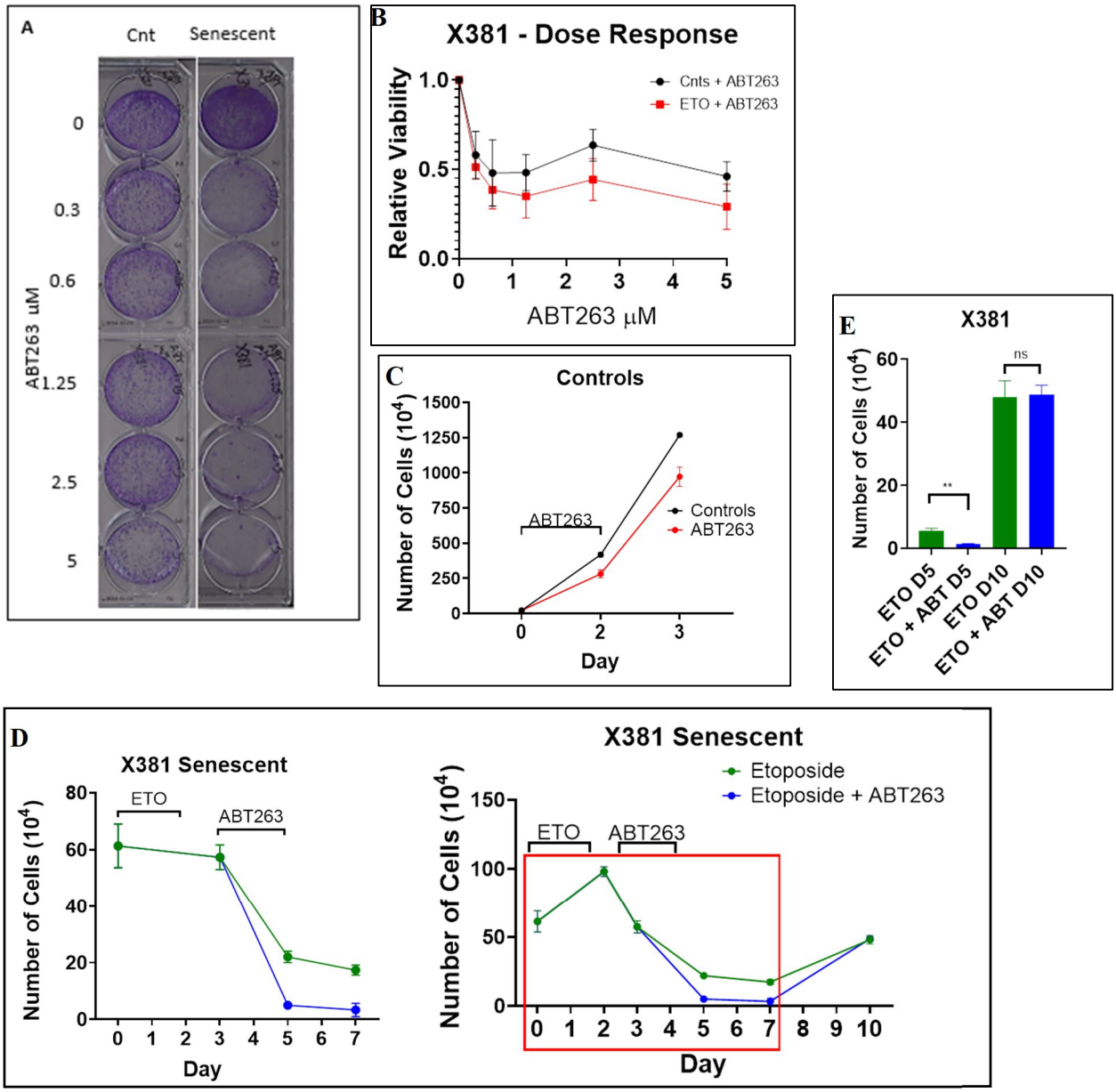

Fig. 13. X381 sensitivity to senolytic ABT263. (A) Crystal violet assay showing a dose response for ABT263. (B) Quantification of the crystal violet using ImageJ. (C) Cell viability time courses for X381 of controls and ABT263 only; (D) Cell viability after treatment of ETO and/or ETO + ABT263 and a close up look of the effect of ABT263 to clarify the response of ABT263. (E) A bar graph to compare ETO to ETO + ABT treatments on days 5 and 10. $^{**}P \leq 0.0012$ indicate statistical significance of treated condition compared to their counterpart as determined using unpaired, Student's *t*-test. All images and line graphs are representative images or graphs from three independent experiments ($n = 3$). Bar graph is mean ± SEM from three independent experiments ($n = 3$).

To examine how much cell death in induced by ABT263, an Annexin-APC/7-AAD staining was assessed (fig. 14), it was observed that there was approximately a 20% increase of cell death with the treatments of ETO + ABT263. With controls and senescent cells, there is the same amount of early apoptosis and when cells are treated with ABT253 only or ETO only, there is more late apoptosis that is observed; furthermore, when the cells are treated with both ETO+ABT263, there is an increase of late apoptosis.

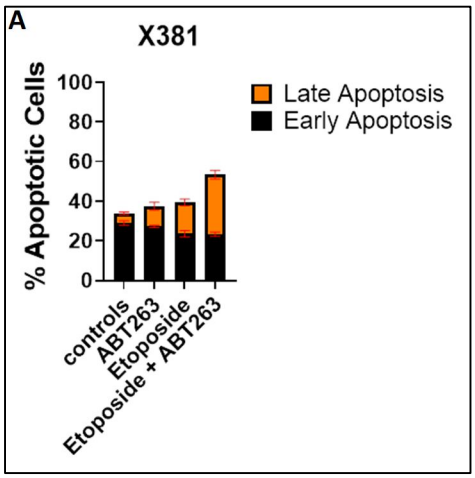

Fig. 14. ABT263 induces apoptotic cell death in senescent cells X577. (A) X577 is Annexin-V/PI quantification of apoptosis induced by 2 μM ABT263 with overnight exposure. Quantification graphs are mean ± SEM from three independent experiments (*n = 3*).

3.11. Senescence induction in syngeneic murine lung cancer cell line, Y143

Figure 15, Y143 doesn't enter senescence and β-gal quantification (fig. 15B) shows a non-significant level of β-gal positive cells. In order to compare these cells with other cell lines that have significant senescence induction, sensitivity to ABT263 was investigated.

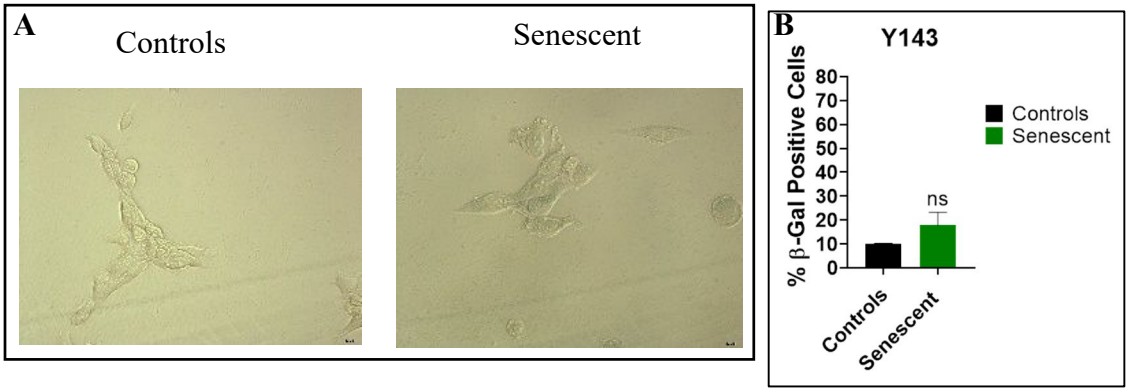

Fig. 15. Etoposide induced senescence in mouse lung cancer Y143 cells. Cells were exposed to ETO (2 μM for 48 hrs) and were evaluated for their increased expression of SA-β-gal using (A) X-gal (bright-field images, objective 20X) or (B) C_{12}FDG, the next day. ns $P \leq 0.2294$ indicates no statistical significance of treated condition compared to controls as determined using unpaired, Student's *t*-test. All images are representative images from three independent experiments (*n = 3*), and quantitative graphs are mean ± SEM from three independent experiments (*n = 3*).

3.12. Y143 sensitivity to ABT263

ABT263 dose responses were obtained (fig. 16). It was concluded from the dose responses that Y143 doesn't respond to ETO or ABT263. This indicates that when the cells do not senesce, ABT263 will have no effect on them.

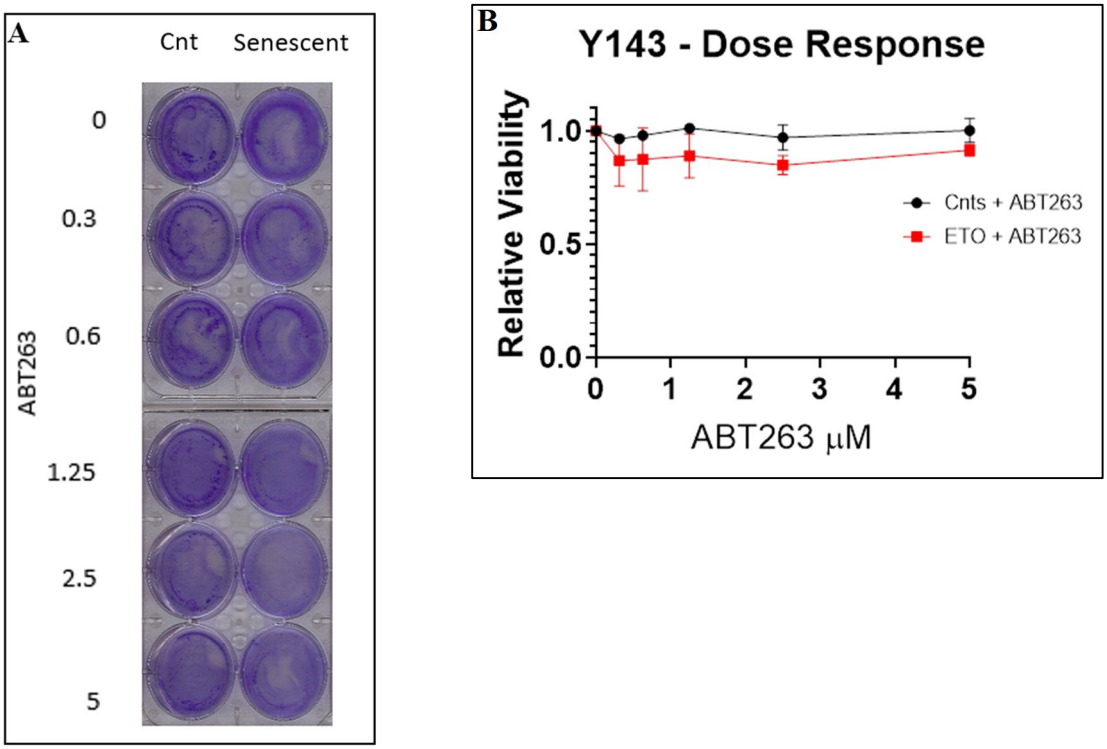

Fig. 16. Y143 sensitivity to senolytic ABT263. (A) Crystal violet assay showing a dose response for ABT263. (B) Quantification of the crystal violet using ImageJ. All images and line graphs are representative images or graphs from three independent experiments (*n = 3*).

3.13. Senescence induction in the syngeneic murine lung cancer cell line, X911

X911 cells show a significant level of senescence induction, in sup. fig. 2, due to the increase in β-gal staining. Unfortunately, these cells were detaching from plates and no further investigation were performed using them.

Sup. Fig. 2. Etoposide induced senescence in mouse lung cancer X911 cells. Cells were exposed to ETO (2 μM for 48 hrs) and were evaluated for their increased expression of SA-β-gal using (A) X-gal (bright-field images, objective 20X) or (B) C_{12}FDG, the next day. **** $P < 0.0001$ indicates statistical significance of treated condition compared to controls as determined using unpaired, Student's *t*-test. All images are representative images from three independent experiments ($n = 3$), and quantitative graphs are mean ± SEM from three independent experiments ($n = 3$).

3.14. Summary of observations

Cell lines with significant senescence induction are, from highest senescence induction to lowest: CMT167, X911, X381, E889, and X577. Y143 cells did not have a significant senescence induction. Table 1 compares all mouse cell lines. Ordering the cell lines from highest to lowest sensitivity to ABT263, based on increase in % apoptosis increase from controls on day 4: X577, E889, CMT167, and X381.

Cell line	% Senescence	ETO - Number of cells (10^4) on D5	ETO+ABT - Number of cells (10^4) on D5	% Reduction from ETO+ABT to ETO on D5	ETO - Number of cells (10^4) at end-of-treatment	ETO+ABT - Number of cells (10^4) at end-of-treatment	% Reduction from ETO+ABT to ETO at end-of-treatment	Increase in % Apoptotic cells on D4
X577	37	14.75	2.5	83.1	149.75 (D10)	78.25 (D10)	47.7 (D10)	56.24
E889	44.2	2.7	0.25	90.7	55.25 (D12)	57.75 (D12)	-4.5 (D12)	42.00
X381	56.9	22	5	77.3	48.00 (D10)	48.00 (D10)	0 (D10)	19.45
CMT167	80	6	1.35	77.5	99.60 (D14)	76.00 (D14)	23.7 (D12)	24.20
Y143	17.8	-	-	-	-	-	-	-
X911	69	-	-	-	-	-	-	-

Table 1. Comparison between cell lines. Senescence induction, number of cells on days 5 and on end of treatment (day 10/12/14), % reduction was calculated by dividing ETO+ABT by ETO, and increase of % apoptosis by Annexin on D4 is the % apoptosis of 48 hrs of ETO exposure and 24 hrs of ABT263 exposure compared to controls.

3.15. Etoposide and ABT263 effects on protein levels

In order to understand how the treatments of ETO and/or ABT263 effects the protein levels, to learn how the proteins induce apoptosis and at what levels of proteins are needed to induce apoptosis, time-course of western blotting were performed using cell lines X577 and E889. Figure 17. X577 cells show an up regulation of the BCL_2 family anti-apoptotic proteins (BCL_2, BCL_{XL}, and BCL_W), particularly BCL_{XL}, after the treatment of ABT263 and/or ETO, this suggests that these proteins are upregulated due to cellular stress from chemotherapeutic drugs. Pro-apoptotic proteins (Bak and Bax) are up regulated with the treatments of ETO and/or ABT263, this denotes the potential activation of cellular apoptosis pathway after senescence induction and the treatment of ABT263. BH3-only proteins (Noxa and Bim) have also been up regulated after the treatment of ETO and ABT263, allowing pro-apoptotic proteins to activate the apoptosis pathway. E889 cells, fig. 18, there is a slight up regulation of the anti-apoptotic proteins after drug treatment, especially after the induction of senescence. Bak is down regulated when treated with ABT263 only and when treated with ETO on days 2 and 3, this may imply that the cells aren't dying, between days 2 and 3 as much as on day 4 with the treatment of ETO

alone, and this is also observed in western blotting of cleaved caspase 3, figure 11B and C. On day 4 of ETO and the combination of ETO and ABT263, there is a down regulation of Bak with the treatments of ABT or ETO only, it up-regulated on day 4 of ETO only and with the treatments of ETO + ABT indicating cells may have activated apoptosis. Bax is slightly up regulated with the treatment of ETO on day 2 and it goes back to its control tone indicating Bax doesn't play a role on cellular apoptosis in this cell line, with the up regulation of Bak on day 4 of ETO only and the combination of ETO and ABT263, increases the levels of cellular death due to the presence of more pro-apoptotic proteins. BH3 proteins, Bim and Noxa, are present in control cells and cells treated with ABT263 only and ETO only and are slightly up-regulated on day 4 and as well as with the combination, signifying the promotion of cellular apoptosis.
In conclusion, when cells are treated with ETO they enter intracellular stress and consequently senescence, which up regulates p53, figures 6C and 9C, this would then up regulate and activate BH3-only proteins. With the up regulation of BH3-only proteins and the accumulation of pro-apoptotic proteins along with the inhibition of pro-survival proteins, the cells endure cellular apoptosis. In conclusion, the changes from western blotting are inconsistent and cannot draw any definitive conclusion. Figure 22 illustrates the pathway when cells are treated with ETO and/or ABT263.

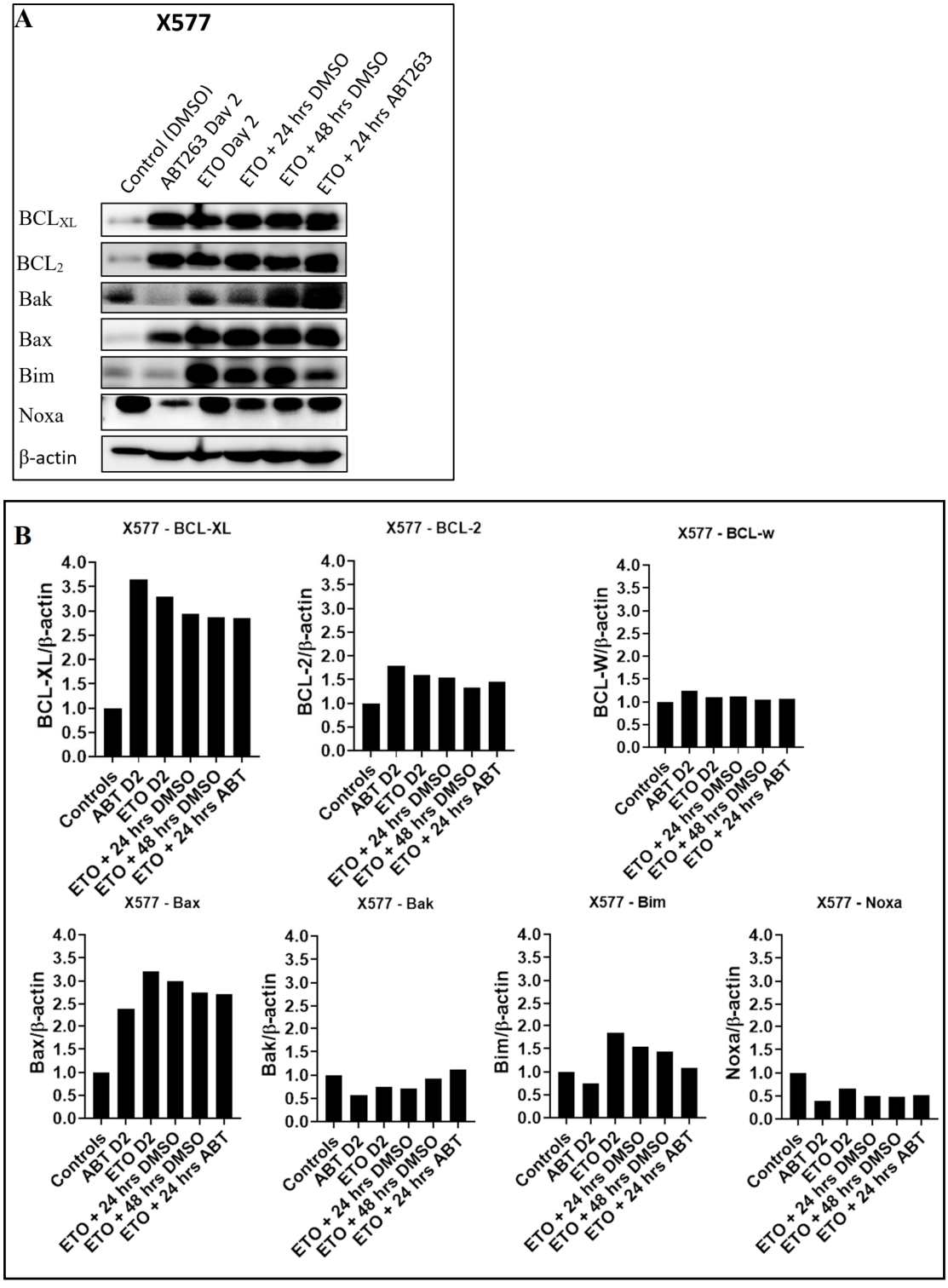

Fig. 17. ABT263 selectivity for BCL_2 , BCL_{XL}, and BCL_W. (A) X577 western blotting for indicated treatments of BCL_{XL}, BCL_2, Bak, Bax, Bim, Noxa, and β-actin. (B) Western blots quantifications normalized to β-actin using ImageJ. Western blots and quantifications are one repeat (*n = 1*).

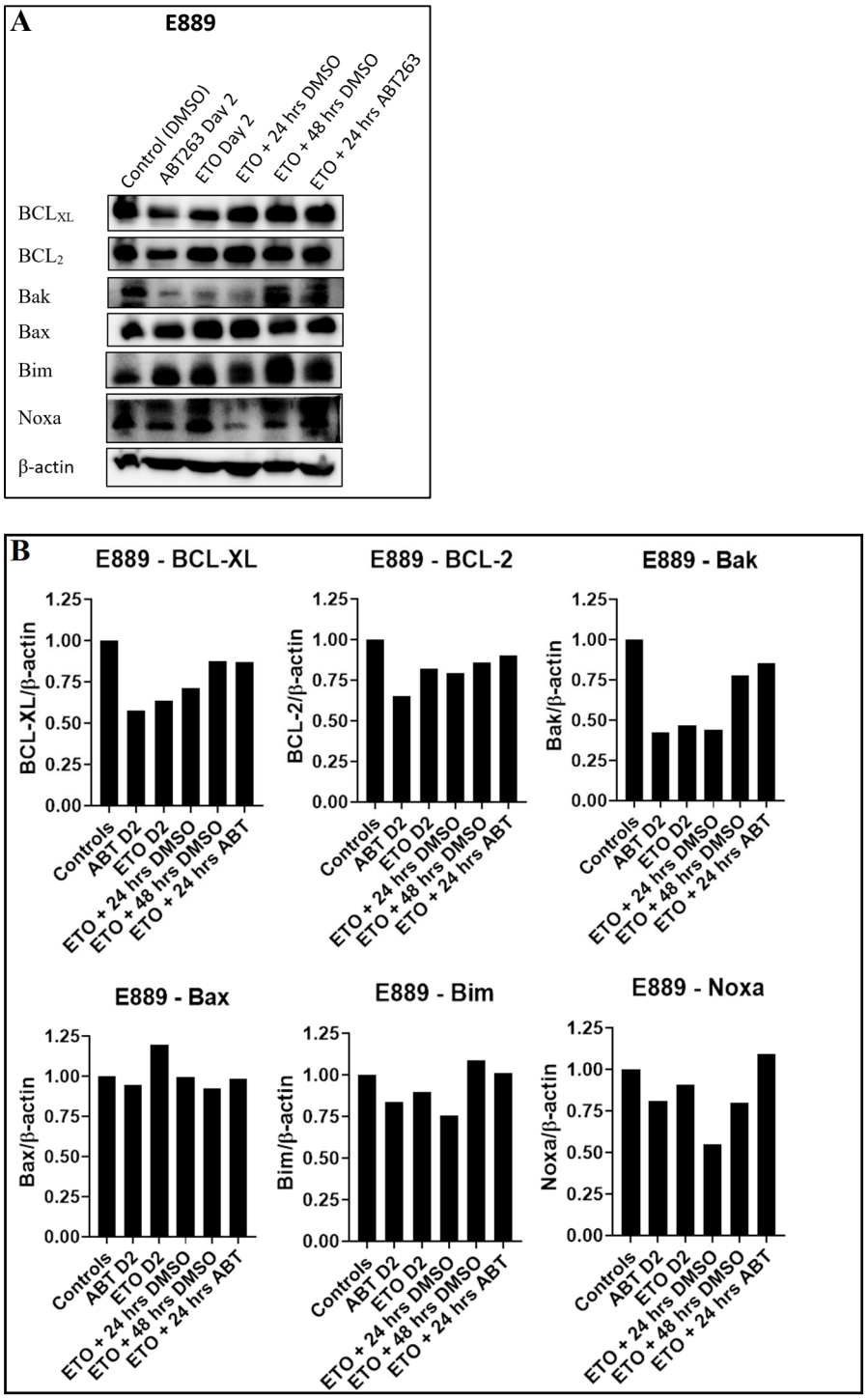

Fig. 18. ABT263 selectivity for BCL_2 and BCL_{XL}. (A) E889 western blotting for indicated treatments of BCL_{XL}, BCL_2, Bak, Bax, Bim, Noxa, and β-actin. (B) Western blots quantifications normalized to β-actin using ImageJ. Western blots and quantifications are one repeat (*n = 1*).

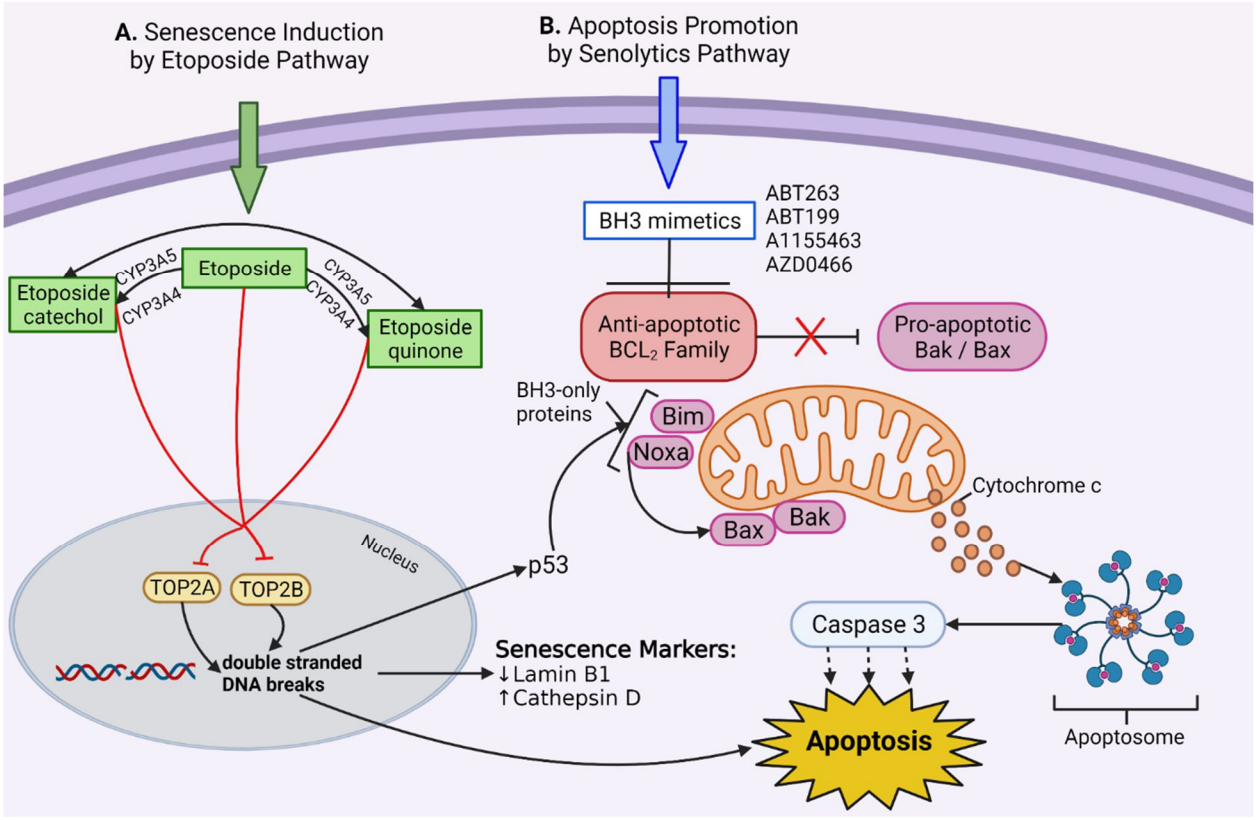

Fig. 22. Etoposide (ETO) and BH3-mimetics pathways. (A) senescence induction by ETO pathway. CYP3A4/5 metabolizes ETO to the O-demethylated metabolites (catechol and quinone). These metabolites and the parent drug, ETO, inhibit topoisomerase II causing double stranded DNA breaks and thus placing the cell in intracellular stress and consequently inducing senescence. (B) Apoptosis promotion by BH3 mimetic drugs. BH3 mimetics inhibit anti-apoptotic proteins (BCL_2, BCL_{XL}, and/or BCL_W) prohibiting them from inhibiting pro-apoptotic proteins (Bak and Bax). From cellular stress and senescence, p53 is up regulated and activates BH3-only proteins (Bim and Noxa). The pathway was created using BioRender.com.

3.16. ABT263 specificity between the BCL_2 family proteins

BCL_2 family members regulate the survival of cells, ABT263 is a BH3 mimetic that inhibits BCL_2 proteins prohibiting them from biding to pro-apoptotic proteins, such as Bak and Bax. To investigate whether ABT263 exerts its effects by inhibiting BCL_{XL} or BCL_2. X577, E889, and X381 cells were chosen to study the effects of ABT199 or A1155463. A1155463 is a BCL_{XL}-specific inhibitor and ABT199 is a BCL_2-specific inhibitor (Leverson et. al., 2015). Those three cell lines were chosen because of their senescence induction levels and their sensitivity to ABT263. After the cells senesced, they were treated with either A1155463 or ABT199 on day three for 48 hours, following the same time-line as ABT263.

X577 cells, figure 19A, shows that ABT263 may exerts its effects by targeting BCL_{XL}, however, it is not clear, and more investigation is needed. E889, figure 19B, clearly shows that ABT263 exerts its effects by targeting BCL_{XL}, because both ABT263 and A1155463 follow the exact trend of response to the drugs. X381 cells, figure 19C, illustrates that ABT263 induces its effects by targeting mostly BCL_{XL}, nonetheless, further investigation is needed for certainty.

To further investigate the ABT263 mechanism in cell lines X577 and X381, cells were treated with first, ETO for 48 hrs, second on day 3, a single treatment of ABT199, the specific BCL_2 inhibitor, with the specific BCL_{XL} inhibitor, A1155463, figure 20. E889 sell line was not chosen to test this synergic treatment because it was clear that ABT263 induces apoptosis by targeting BCL_{XL}. It was observed that cells treated with ETO + ABT199 + A1155463, following the same treatment from ABT263, aren't affected to the synergic triple drug treatment as ETO + ABT263. This suggests that ABT263 targets another protein in addition to BCL_{XL} and BCL_2, which is BCL_w.

In conclusion, ABT263, has been found to target BCL_{XL} only in E889 cells as well as targeting BCL_{XL}, BCL_2, and/or BCL_W in X577 and X381 cells to induce its senolytic effects.

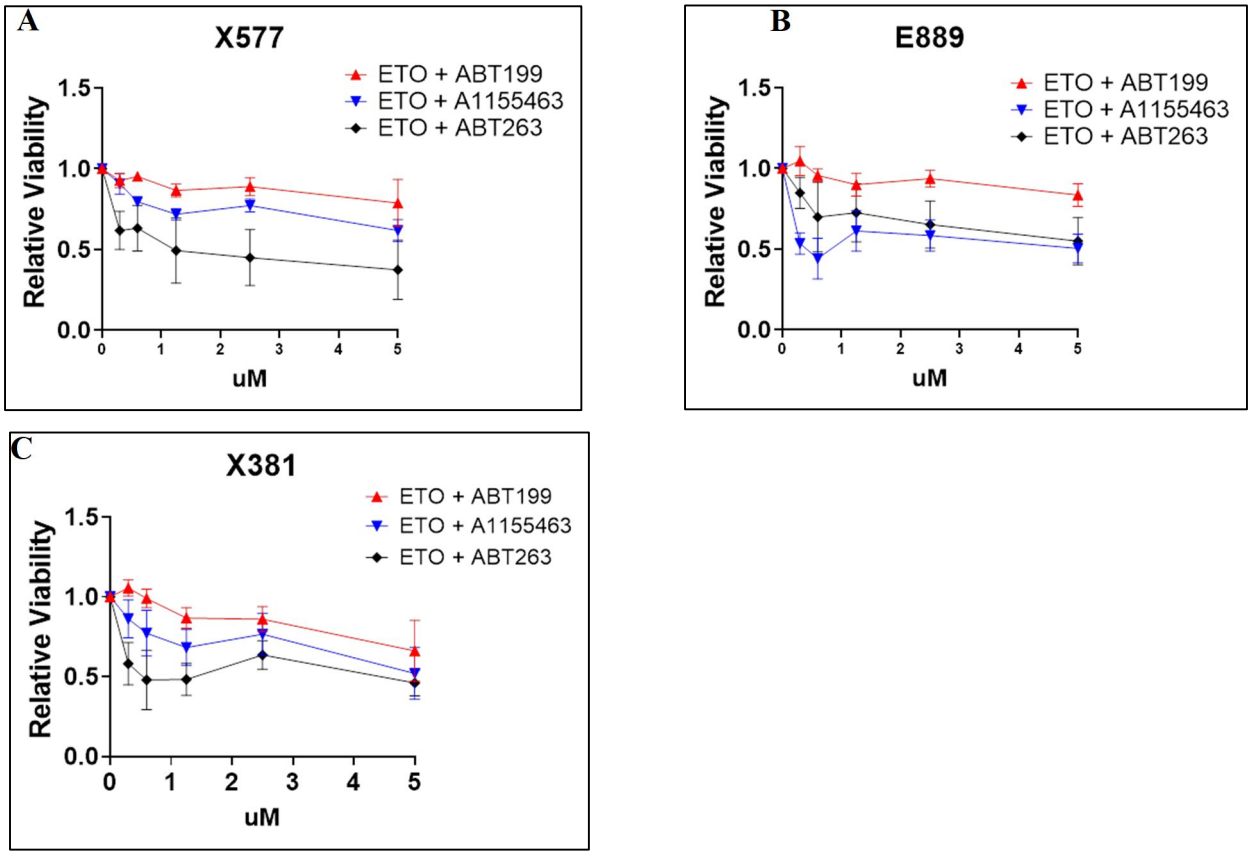

Fig. 19. ABT263 selectivity between BCL_2 or BCL_{XL} in X577, E889, and X381. (A) X577 quantification for crystal violet dose response to ABT199 or A1155463 compared to ABT263. (B) E889 quantification for crystal violet dose response to ABT199 or A1155463 compared to ABT263. (C) X381 quantification for crystal violet dose response to ABT199 or A1155463 compared to ABT263. Lines graphs are mean and error ± SEM from three independent experiments (*n = 3*).

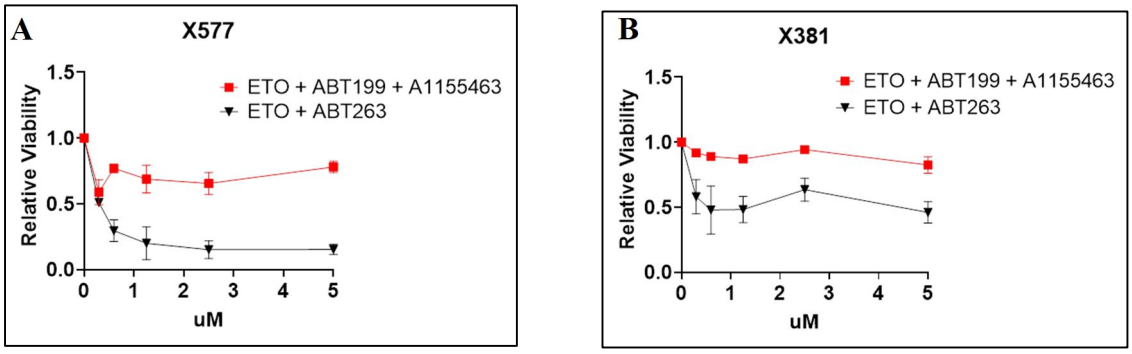

Fig. 20. ABT263 selectivity between BCL_2 and BCL_{XL} in X577 and X381. (A) X577 quantification for crystal violet dose response to ETO + ABT199 + A1155463 compared to ETO + ABT263. (B) X381 quantification for crystal violet dose response to ETO + ABT199 + A1155463 compared to ETO + ABT263. Lines graphs are mean and error ± SEM from three independent experiments (*n = 3*).

3.17. ARV825 sensitivity

To broaden the scope of choices to induce cell death in senescent cells, the inhibition of BET family protein was investigated. To investigate BET inhibitor, ARV825, on murine lung cell lines Y856, X577, X381, and E889. Non-senescent cells were treated with ARV825 with different doses of ARV825 for 48 hours (100, 50, 25, 12.5, 6.25 and 0 nM) and were replenished for another 48 hours using the same doses; and senescent cells were treated with ARV825 the as the non-senescent were, on day 3 ARV825 was added for 48 hours, with indicated concentrations, and ARV825 was replenished for another 48 hours using the same doses. From the crystal violet dose response (figure 21) it was concluded in these cell lines ARV825 does not induce cellular apoptosis and therefore it cannot be used in these cellular models.

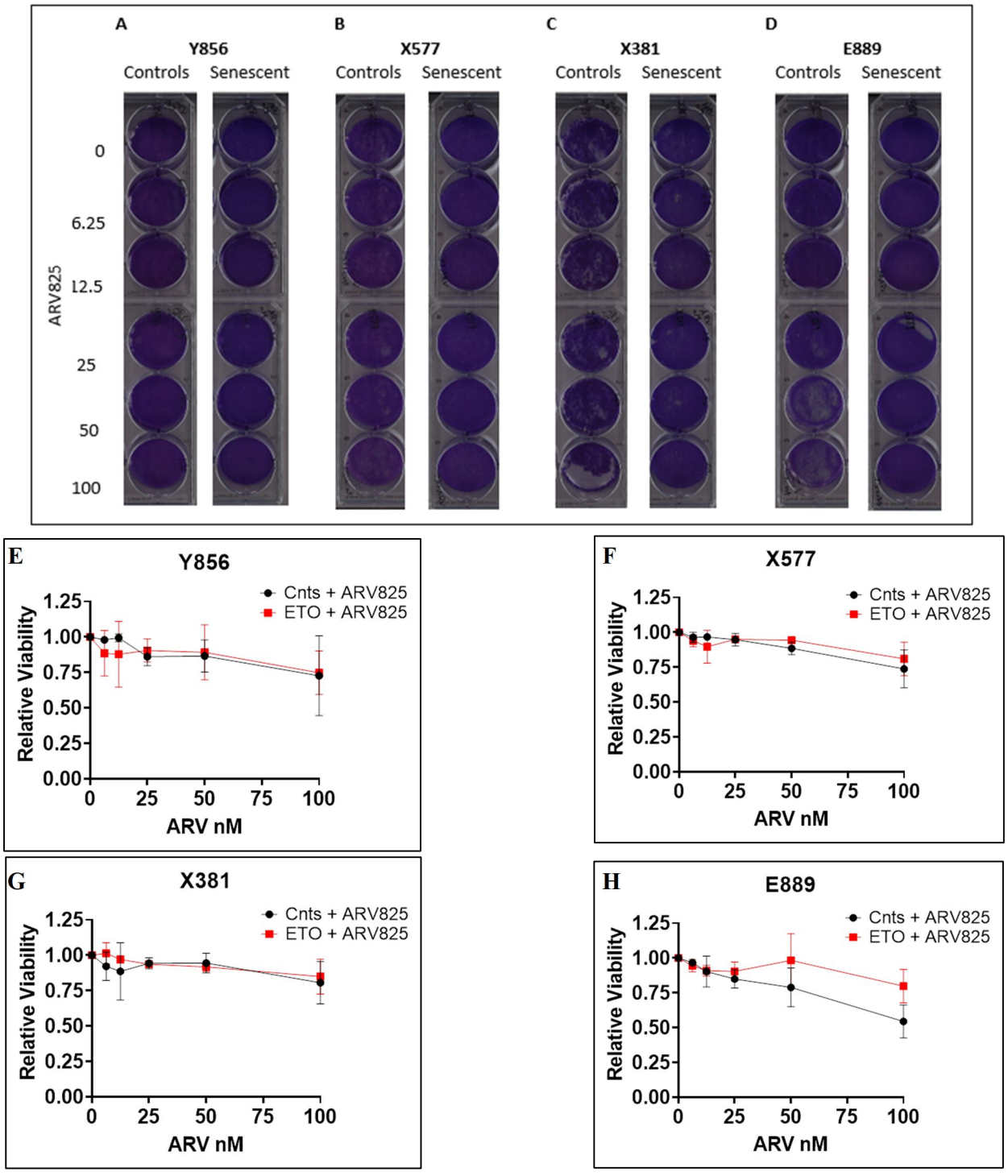

Fig. 21. Sensitivity to ARV825. (A, B, C, D) Crystal violet assay showing a dose response for ARV825 in lines Y856, X577, X381, and E889, respectively. The highest dose of treatment was 100 nM and the lowest was 0 nM, we treated with ARV825 for 48 hours and replenished the treatment for another 48 hours. (E, F, G, H) are quantification graphs of dose responses using ImageJ. All images are representative images from three independent experiments ($n = 3$) and graphs are mean ± SEM from three independent ($n = 3$).

4. Discussion

The hypothesized approach of a two-step treatment for cancer cells with first a senescence inducer followed by a senolytic has shown to be a potential treatment for cancer (Robbins, et. al., 2020). The induction of senescence has proved to be a useful outcome in the treatment of cancer and for many years the production of senescence induction agents has been encouraged (Nardella et. al., 2011). Nevertheless, senescent cells have been identified as contributors to tumorigenesis by promoting many hallmarks of cancer, including evasion of the immune system (Prieto et. al., 2019). There are other senescence inducers that have been tested in other cellular models like cisplatin and doxorubicin (Saleh et. al., 2020; Ahmadinejad et. al., 2022). Other senescence inducers may induce different degrees of senescence which can be a more profound or less profound. This emphasizes the importance to use senolytics to clear senescent cells.

In this study, it was observed that non-small cell lung cancer cells were induced into senescence by ETO. The cells were enlarged and were more granulated from the CCFs and demonstrated β-gal staining, and up-regulation of p53 and p21. Senescent cells that were treated with ABT263 were driven into apoptosis as shown by plasma membrane structural changes that include the translocation of phosphatidylserine from the inner to the outer leaflet (extracellular side) of the plasma membrane, which was analyzed after Annexin V/PI staining.

The hypothesis of this work was different cell lines will have different degrees of senescence and that the magnitude of the response to senolytics would reflect the extent of senescence induction. The cell lines that were induced into senescence were, from highest level of senescence to lowest, CMT167, X911, X381, E889, X577, and Y143. To order the cells lines that respond to ABT263 from highest percent reduction to lowest on day 5: E889, X577, CMT167, and X381. To order the same cell lines at the end-of-treatment (end of time-course) based on percent reduction: X577, CMT167, X381, and E889. Based on the precent apoptosis increase from controls on day 4 that is induced by the Annexin V staining, cells with the highest percent apoptosis to lowest, X577, E889, X381, and CMT167. In conclusion, there is no correlation between the degrees of senescence and the magnitude of the response to senolytic, ABT263.

Cell line	% Senescence positive	% Reduction (D5)
X577	37	83.1
E889	44.2	90.7
X381	56.9	77.3

One reason behind this lack of correlation between the magnitude of senescence induction and the response to the senolytic, ABT263, can be the different mutations each cell line has. X577 cell line was derived from a male mouse and has *Kras*^{G12D} and *Smad4*$^{+/-}$. E889 cell line was derived from a male mouse and has *Kras*^{G12D}, *Map3K7*$^{-/-}$, and *GFP*$^{+}$. X381 cell line was derived from a male mouse and has *Kras*^{G12D}, *PTEN*$^{+/-}$, *p53*$^{+/-}$, and *GFP*$^{+}$. Y143 cell line was derived from a female mouse and is a EML4-ALK mutant cell line.

From previous work (Saleh et. al., 2020), ABT263 induced its senolytic effects by targeting BCL_{XL}, moreover, from work in this project, ABT263 may induce its senolytic effects by targeting BCL_{XL} in E889 and more than one BCL_2 family member in X577 and X381.

One possible approach to improve the response to treatment with ETO and ABT263 would be for the X577 cells to be re-induced into senescence with the exposure of ETO and re-treated with ABT263. This may keep the cells in a steady-state of senescence and clear more cells after the use of the senolytic, which may give a longer remission period. X381 cells stayed in senescence the longest, compared to the other cell lines tested, and in order to clear more senescent cells, the cell may need to be treated with multi-treatments of the senolytic, which would delay the cancer cells' recovery from senescence when treated with ETO and ABT263.

5. Future directions

Different cell lines respond differently to therapy due to their genetic makeup; furthermore, for future research, learning how cancer cell lines differ from each other genetically may help provide guidance as to why they respond differently to therapy. Additionally, why some senescent cells respond to BCL_2 family inhibitors (ABT263) but not BET family protein degrader (ARV825) ought to be investigated.

One of our goals was to determine how the immune system will interact with NSCLC cells when treated with a senescence-inducer and a senolytic. In this study, there is one cell line that has potential use for in vivo studies, X577, using ETO and ABT263 as the drugs of choice. X577 cells respond to ABT263 by up-regulating mostly BCL_{XL}, however, when treated with selective BCL_2 or BCL_{XL} or both, it appeared to have not responded to the senolytics as well as to ABT263. This may be because ABT263 targets a combination of more than one BCL_2 family protein other than BCL_2 and BCL_{XL} only.

Citations

Acosta, J. C. (2013, August). A complex secretory program orchestrated by the inflammasome controls paracrine senescence. PubMed. https://pubmed.ncbi.nlm.nih.gov/23770676/

Ahmadinejad, F. (2022, March). Senolytic-Mediated Elimination of Head and Neck Tumor Cells Induced Into Senescence by Cisplatin. PubMed. https://pubmed.ncbi.nlm.nih.gov/34907000/

American Cancer Society. (2020, May 27). *Non-small cell lung cancer chemotherapy | Chemo side effects*. American Cancer Society | Information and Resources about for Cancer: Breast, Colon, Lung, Prostate, Skin. Retrieved April 8, 2022, from https://www.cancer.org/cancer/lung-cancer/treating-non-small-cell/chemotherapy.html

Campisi, J. (2001, November 1). Cellular senescence as a tumor-suppressor mechanism. https://www.cell.com/trends/cell-biology/fulltext/S0962-8924(01)02151-1?_returnURL=https%3A%2F%2Flinkinghub.elsevier.com%2Fretrieve%2Fpii%2FS0962892401021511%3Fshowall%3Dtrue

Chakradeo, S. (2016). Is senescence reversible? PubMed. https://pubmed.ncbi.nlm.nih.gov/26302802/

Chang, J. (2016, January). Clearance of senescent cells by ABT263 rejuvenates aged hematopoietic stem cells in mice. PubMed. https://pubmed.ncbi.nlm.nih.gov/26657143/

Debacq-Chainiaux, F. (2009, November 19). Protocols to detect senescence-associated beta-galactosidase (SA-βgal) Activity, a biomarker of senescent cells in culture and in vivo - Nature protocols. Nature. https://www.nature.com/articles/nprot.2009.191

Dorr, J. R. (2013, August 14). Synthetic lethal metabolic targeting of cellular senescence in cancer therapy. PubMed. https://pubmed.ncbi.nlm.nih.gov/Gorgoulis, V. (2019, October 31). Cellular Senescence: Defining a Path Forward. www.cell.com. https://www.cell.com/cell/fulltext/S0092-8674(19)31121-3?_returnURL=https%3A%2F%2Flinkinghub.elsevier.com%2Fretrieve%2Fpii%2FS0092867419311213%3Fshowall%3Dtrue

Hanahan, D. and Weinberg, R. A. (2011, March 4). *Hallmarks of Cancer: The Next Generation*. https://www.cell.com/fulltext/S0092-8674(11)00127-9

Hande, K. R. (1998, April 1). *Etoposide: Four decades of development of a topoisomerase II inhibitor*. ScienceDirect.com | Science, health and medical journals, full text articles and books. https://www.sciencedirect.com/science/article/pii/S0959804998002287?casa_token=3IRY2Y51_qMAAAAA:0R8PeSLAmawky5CiIASj2yUFdT8HuBTd4-MM0CG-xhcgdJ2Ab3pzdVrYhFT7ZcaA651yCA0k

Hernandez-Segura, A. (2018, June). *Hallmarks of Cellular Senescence*. PubMed. https://pubmed.ncbi.nlm.nih.gov/29477613/

Khushboo, K. (2015, January 28). A novel cytostatic form of autophagy in sensitization of non-small cell lung cancer cells to radiation by vitamin D and the vitamin D analog, EB 1089. Taylor & Francis. https://www.tandfonline.com/doi/full/10.4161/15548627.2014.993283

Lawen, A. (2003). Apoptosis - an introduction. *BioEssays*. https://onlinelibrary.wiley.com/doi/10.1002/bies.10329

Leverson, J. D. (2015, March 18). *Exploiting selective BCL-2 family inhibitors to dissect cell survival dependencies and define improved strategies for cancer therapy*. PubMed.

Munoz-Espin, D., & Serrano, M. (2014, June 23). Cellular senescence: from physiology to pathology. https://www.nature.com/articles/nrm3823

Nardella, C.(2011, June 24). *Pro-senescence therapy for cancer treatment*. PubMed. https://pubmed.ncbi.nlm.nih.gov/21701512/
NIH: National Cancer Institute. (2021, August 27). *Lung cancer—Patient version*. National Cancer Institute. Retrieved April 8, 2022, from https://www.cancer.gov/types/lung
Patterson, C. M. (2021, January 25). Design and optimization of dendrimer-conjugated bcl-2/xL inhibitor, AZD0466, with improved therapeutic index for cancer therapy - Communications biology. Nature. https://www.nature.com/articles/s42003-020-01631-8
Petrova, N. V. (2016, December). Small molecule compounds that induce cellular senescence. PubMed. https://pubmed.ncbi.nlm.nih.gov/27628712/
Prasanna, P. G., (2021, April 1). *Therapy-induced senescence: Opportunities to improve Anticancer therapy*. PubMed Central (PMC). https://www.ncbi.nlm.nih.gov/pmc/articles/PMC8486333/
Prieto, L. I. (2019, June 18). *Cellular senescence and the immune system in cancer*. Karger Publishers. https://www.karger.com/Article/Abstract/500683
Robbins, P. D. (2020, September 30). *Senolytic drugs: Reducing senescent cell viability to extend health span*. PubMed Central (PMC). https://www.ncbi.nlm.nih.gov/pmc/articles/PMC7790861/
Saleh, T. (2020, July 11). *Clearance of therapy-induced senescent tumor cells by the senolytic ABT-263 via interference with BCL-XL–BAX interaction*. FEBS Press. https://febs.onlinelibrary.wiley.com/doi/full/10.1002/1878-0261.12761
Sharpless, N. E., & Sherr, C. J. (2015, June 24). Forging a signature of in vivo senescence. www.nature.com. https://www.nature.com/articles/nrc3960
Short, S. (2019, March). Senolytics and senostatics as adjuvant tumour therapy. PubMed. https://pubmed.ncbi.nlm.nih.gov/30737084/
Wakita, M. (2020, April 22). *A BET family protein degrader provokes senolysis by targeting NHEJ and autophagy in senescent cells*. PubMed Central (PMC). https://www.ncbi.nlm.nih.gov/pmc/articles/PMC7176673/
Wang, L. (2017, October 17). High-throughput functional genetic and compound screens identify targets for senescence induction in cancer. PubMed. https://pubmed.ncbi.nlm.nih.gov/29045843/
Xu, M. (2015, December 19). Targeting senescent cells enhances adipogenesis and metabolic function in old age. PubMed. https://pubmed.ncbi.nlm.nih.gov/
Yang, J., Bongi, A., & Schuetz, E. G. (2009, July). Etoposide pathway. PubMed Central (PMC). https://www.ncbi.nlm.nih.gov/pmc/articles/PMC4164627/
Zhan, Y. (2019, July 23). BH3 mimetic ABT-263 enhances the anticancer effects of apigenin in tumor cells with activating EGFR mutation. BioMed Central. https://cellandbioscience.biomedcentral.com/articles/10.1186/s13578-019-0322-y
Zhu, Y. (2015, August 14). The Achilles' heel of senescent cells: From transcriptome to senolytic drugs. PubMed. https://pubmed.ncbi.nlm.nih.gov/